TRANSFER

Výzkum a vývoj pro letecký průmysl

č 13 / 2010

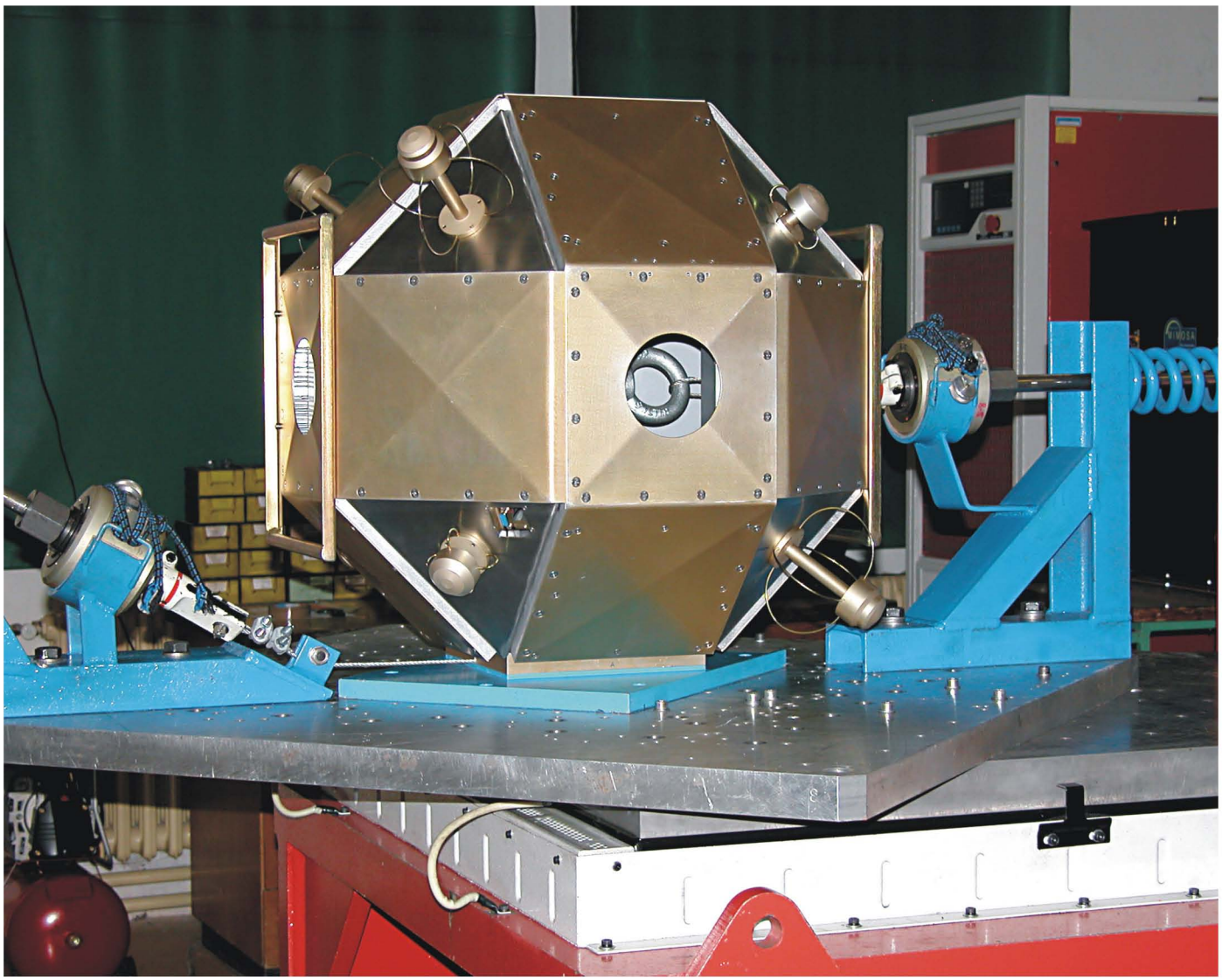

Toto číslo elektronického sborníku obsahuje příspěvky přednesené na mezinárodním semináři - Pokročilé technologie, materiály a zařízení pro kosmické aplikace.
"Advanced technologies, materials and devices for space application"

ISSN 1801 - 9315

VZLÚ, a. s., Beranových 130, 199 05 Praha - Letňany
Tel.: +420 225 115 332, Fax: +420 286 920 930, e-mail: info@vzlu.cz, www.vzlu.cz

TRANSFER

Výzkum a vývoj pro letecký průmysl

Elektronický sborník VZLÚ, a.s.
Číslo 13, říjen 2010, 5. ročník

Adresa redakce:

Výzkumný a zkušební letecký ústav, a.s.
Beranových 130, 199 05 Praha 9, Letňany
Tel.: 225 115 223, fax: 286 920 518

Šéfredaktor:

Ing Ladislav Vymětal (e-mail: vymetal@vzlu.cz)

Technický redaktor, výroba:

Stanislav Dudek (dudek@vzlu.cz)

Vydavatel: Výzkumný a zkušební letecký ústav, a.s.

EUROPEAN UNION
EUROPEAN REGIONAL DEVELOPMENT FUND
INVESTMENT IN YOUR FUTURE

SPACE'2010
International Seminar
"ADVANCED DEVICES, MATERIALS AND RESEARCH METHODS FOR SPACE APPLICATION"
5-7 October 2010
Prague, Czech Republic

* * *

Obsah sborníku / Contents

Dynamic Behavior of Locking Mechanism of Microaccelometer

K. Patocka, T. Jamroz, J. Had, VZLÚ a.s., Prague, Czech Republic

The article describes developing phases of Locking mechanism (LM) of Microaccelerometer (MAC). Because of LM failure during testing appropriate design changes were doing and computational models were developing at the same time to asses LM and its crucial parts. Analyses justified final design solution which succeeded in testing as well.

Introduction

MAC is an instrument to be used for very precise measurement of acceleration. For linear acceleration, its range shall be $\pm 10^{-4} m/s^2$, resolution shall be better than $3.10^{-9} m/s^2$, and accuracy shall be $10^{-8} m/s^2$. For angular acceleration, its range shall be $\pm 9.6\ 10^{-3} m/s^2$, resolution shall be better than $10^{-7} m/s^2$, and accuracy shall be $10^{-8} m/s^2$. It has been finishing for SWARM mission. The most important and complicated mechanical part is LM which locked Sensor. MAC contains three LM, i.e. one for each axis.

The previous version of MAC had difficulties with unlocking due to cold weld in vacuum, thus a new mechanism using fiber was developed based on a lever hold in locked position by fiber. But LM failed during vibration test campaign that time. Performing random vibration fiber Power Pro broke at edges. Filleting helped a little but did not solve the issue so that rollers were deployed instead of edges. But Power Pro failed again and therefore was replaced by Dyneema fiber.

lM current design Description

All important parts of LM are depicted in Fig.1. The Sensor is locked by a Locking Rod. Its position is defined by a Lever arm which has a slot for head of Locking Rod (see also Fig.3). The Lever arm is secured by a fiber that is tightened by a spring. The spring is located between Piston and Cantilever wall. The fiber is fixed on one side by rope at hole of Piston, then goes through the Piston, spring, Cantilever, over rollers to resistors and is ended up by fixing on the other side. After overburning fiber by resistors, the LM is unlocked, because the fiber is pulled out by the spring at piston and other two springs of different diameters (first one inside the second one) lift up the Locking Rod. Once the Locking Rod is lifted up the Sensor is released.
A Lever End Stop on which rollers are mounted (except for one mounted on Lever arm) is not shown in Fig. 1.

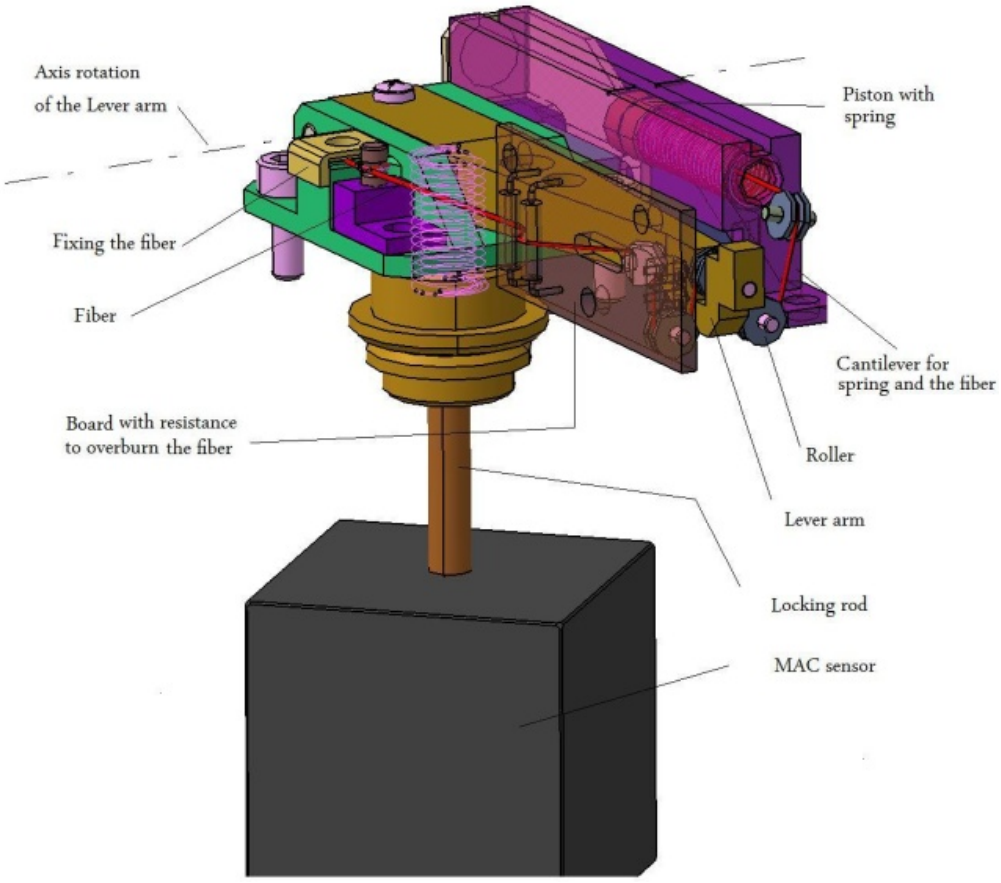

Figure 1 - Basic parts of LM

It's evident that the springs, Locking Rod, Lever and fiber are very important parts. They plays crucial role for right function and ensure reliability of the LM.

Mathematical Models of LM

There were made three models to simulate dynamic behavior of LM. The first simplest one was made in Matlab software. This model consists of rigid parts only. The fiber was replaced by a spring. The model proved that LM is reliable for various dynamic loads. The second model was made in MSC.Adams. The model is the same as the previous one but flexible lever arm was incorporated, so that deformation of the lever arm could be considered. The last model was made in Abaqus in the most precise manner, simulating flexibility of all crucial parts, contacts between parts (with friction between fiber and rollers) etc.

All three models were loaded according to MAC Specification, particularly by the most dangerous random vibration. Random vibration of the MAC shall have been performed with the levels given in the following table, applied to each axis with duration of 120 second in qualification level. The severest load of x axis is depicted in the following table as it was used in analyses (see also blue curve in Fig. 2).

Axis	Frequancy	Aceptance.	Qualification
X	20-100 Hz	+3dB/Oct	+3dB/Oct
	100-300 Hz	0.27 g2/Hz	0.27 g2/Hz
	300-2000 Hz	-5dB/Oct	-5dB/Oct
		12.02 g (RMS)	15.23 g (RMS)

Table 1 - Random environment levels

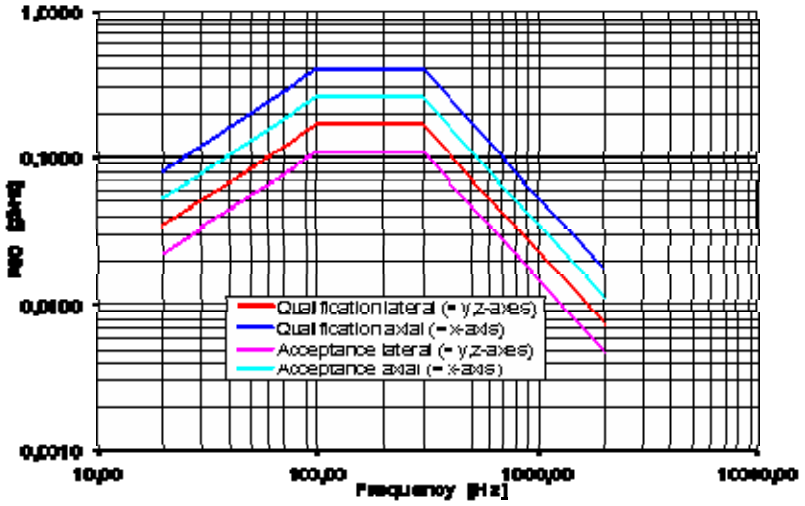

Figure 2 - Random environment levels

Models of LM verifying locking force

The new design of LM in MAC posed issue about stiffness of springs. They were calculated by hand from basic quasistatic analysis considering mass of Sensor and acceleration. Since the most sensitive part – Sensor shall be locked during the whole launch some check analysis had to be done to prove that no loss of locking appeared. For that reason the following models in Matlab and in MSC.Adams were developed. The most important parts influencing locking force were taking into account. The schematic drawing of model is in Fig. 3. All parts are joined to center point where dynamic loads were applied. Contacts were made up between Lever and Locking Rod and between Sensor and Locking Rod at the center point. Hertz rule (continuous force) was used for the contacts. The Lever was joined to center point by rotational joint and the Sensor and the Locking Rod were joined to center point by translational joint. The fiber was replaced by spring. Vibration loading was applied in the centre point for both models.

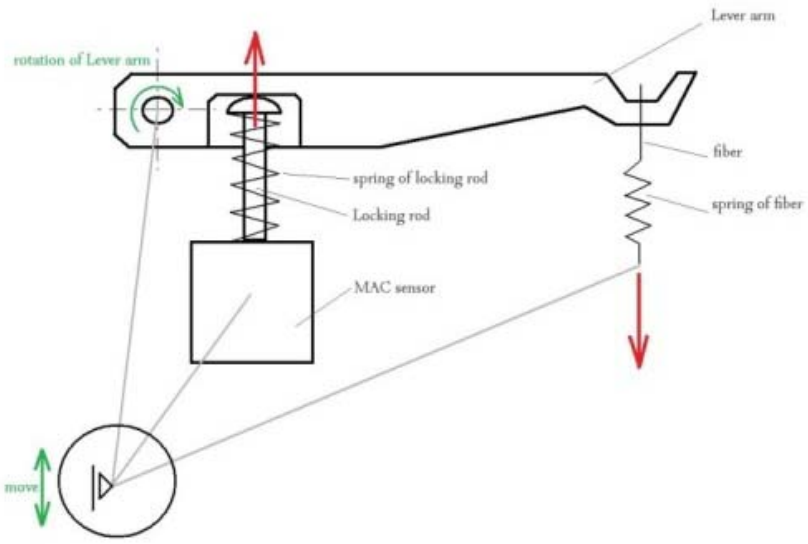

Figure 3 - Simplified model of LM

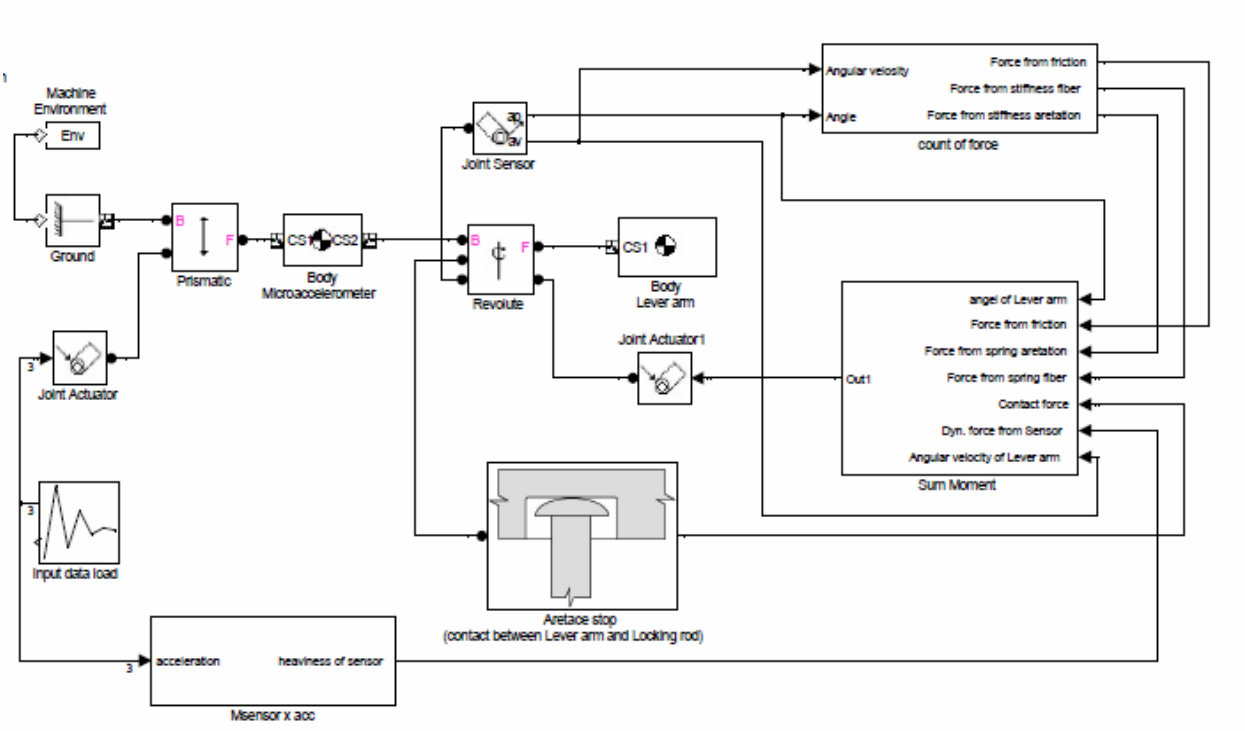

Figure 4 - The diagram of model of LM

Model in Matlab took into account rigid parts as baseline. Toolbox SimMechanics were used for implementation of the model which is shown in Fig. 4.

Rigid Lever was replaced by flexible part in MSC.Adams model. It makes the analysis more precise Locking forces result lesser than the locking forces for the rigid model. And you can also find Lever deformation.

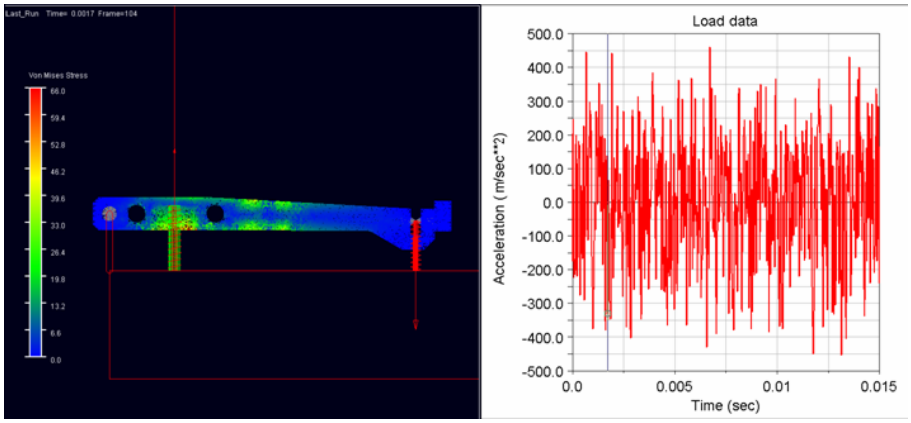

Figure 5 - Model of LM and random load in Adams

Results were similar for both models except for magnitude. You can see it in Fig. 6. It was proven this way that LM reliably locks the Sensor in the course of vibration spectra excitation.

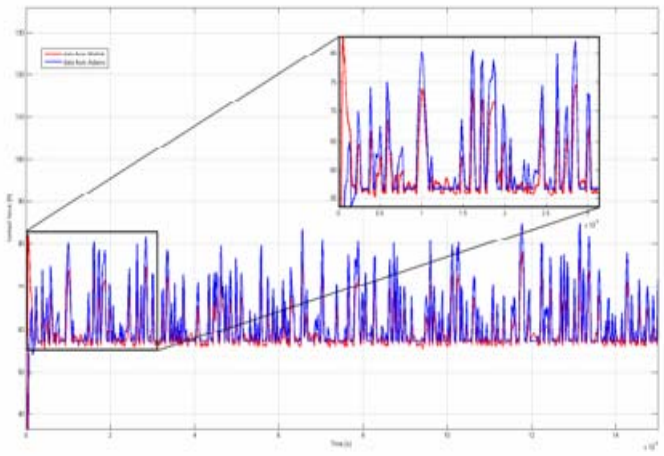

Figure 6 - Comparison of models in Matlab and Adams

FEM model of LM verifying fiber

FEM analyses were done fibers to be checked and considered as reliable. The properties of Dyneema fiber are used in the following analysis.

Model was developed and solved in Abaqus. Since discontinuous effects (contacts and friction) dominate the solution, explicit dynamics approach is often computationally less expensive and more reliable than an implicit quasi-static solution. Next reason for choosing explicit integration schema is possibility to use short time of exciting (e.g. shock spectrum).

Structure of model was adjusted to chosen explicit solution technique. Whole model contains two main families of parts, flexible and rigid body, respectively.

Besides, the model contains other structure parts as point mass or spring elements. FE model is shown in Fig. 7.

Time of solution is given by maximal stable time increment. Rigid body does not affect the stable time increment and therefore as many parts as reasonable use rigid elements. Those parts are all rollers, board with resistors, Locking Rod, Cantilever. Flexible bodies are Lever (4-node linear tetrahedron, i.e. continuum solid elements), Piston (4-node doubly curved shell, finite membrane strains, i.e. structural shell elements) and fiber (2-node truss, linear displacement, i.e. no bending stiffness, element can transmit only axial force). The Sensor was approximated as point mass. All springs (it means spring preloading Piston and spring preloading the Locking Rod) are realized using special elements (in ABAQUS called connector elements) which provide nonlinear stiffness behavior and to which is prescribed nonzero force (pre-stress) and zero deformation.

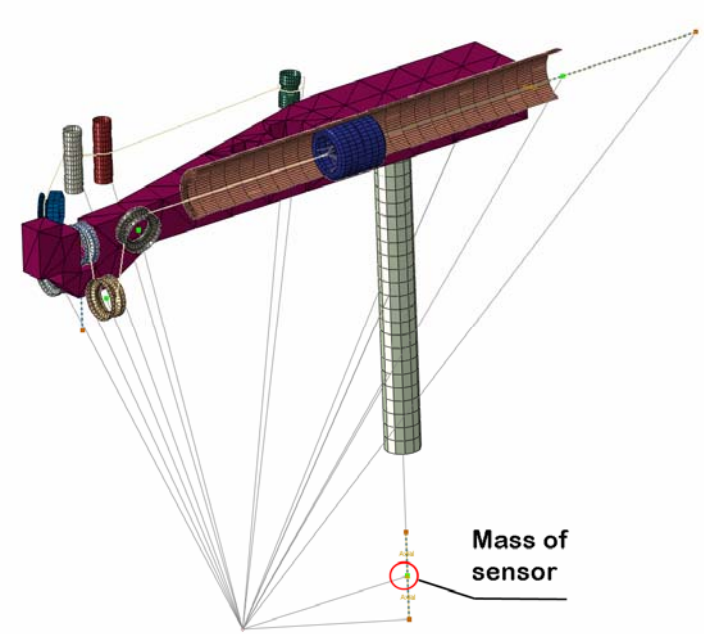

Figure 7 - Overview of FEM model

Parts which are in the real MAC fixed to the structure are attached to the single point (connection represent via constrain equation - coupling constrain) in FE model. Interaction between bodies is based on contact including friction.

Dynamic analysis was carried out with random exciting and dynamic behavior of whole model was verified with experimental data, with measurement of natural frequency respectively. Acceleration response on upper side of lever arm (see Fig. 8) was used to compare resonance frequency. Complete run of analysis can be divided into two phases. In the first one LM is loaded from pre-stress spring and in second one is mechanism excited prescribed loading in common point.

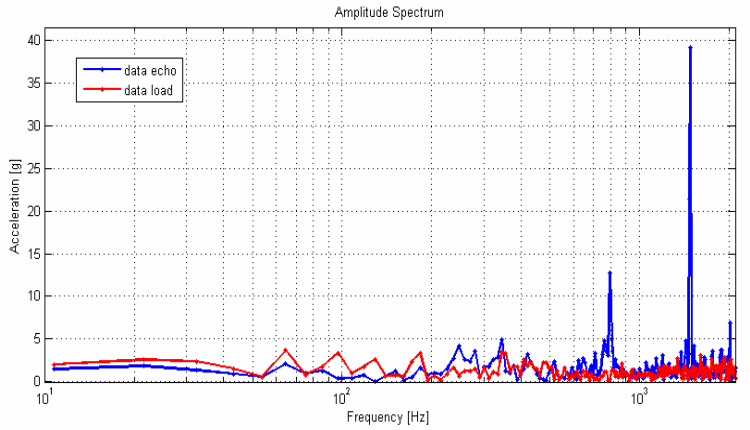

Figure 8 - Acceleration response on Lever

As shown in Fig. 8 and in Tab. 2 first resonance frequency is relatively closed considering the simplification of model.

	Frequency of resonance
Experiment	620Hz
FEM	797Hz

Table 2 - Comparison between test and FEM results

After verifying dynamic behavior of FE model by comparing first resonance frequency, crucial element in fiber was determined based on maximal tensile stress in fiber. Location of the latter element is the same as location of point of failure of former fiber, i.e. behind the first roller from piston side (see also Figs. 9 and 10).

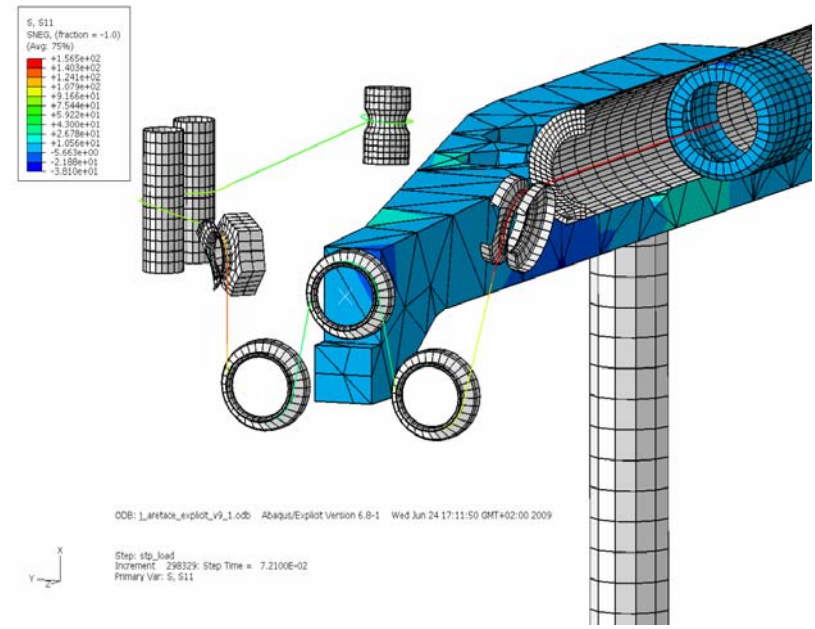

Figure 9 - Stress response of LM (random)

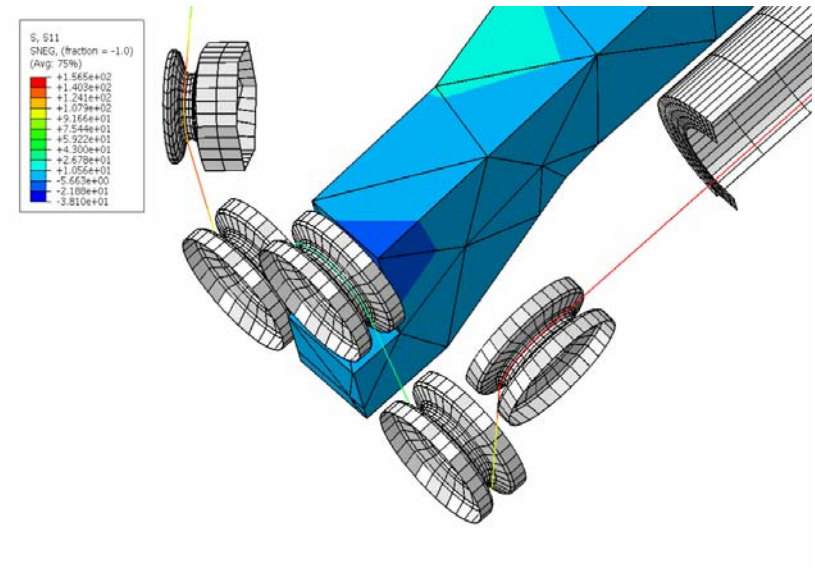

Figure 10 - Stress response of fiber going over rollers (random)

In the following picture is point out stress in fiber during random vibration. Results showed no problem in.

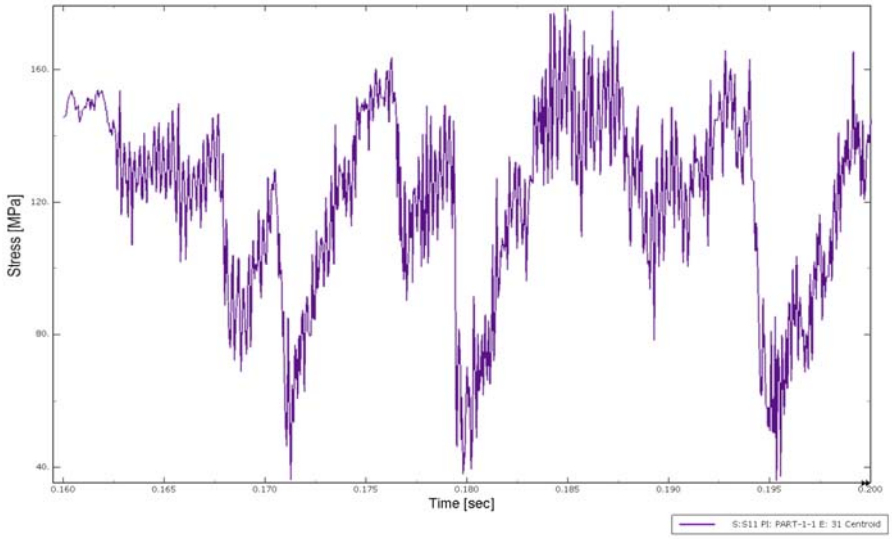

Figure 11 - Stress in the fiber in critical point

Vibration Tests of MAC

Sinus and random vibration tests of the MAC were carried out at the Aeronautical Research and Test Institute (VZLÚ a.s.) in Czech Republic. The tests showed that a critical point of the LM is the fiber. During random vibration test the former Power Pro fiber broke (see Fig. 12) although redesing using rollers was performed. At that point a new fiber (Dyneema) was selected and comprehensive analyses described in previous chapter were done. As their results confirmed ability of new fiber to withstand the vibration new tests were carried out.

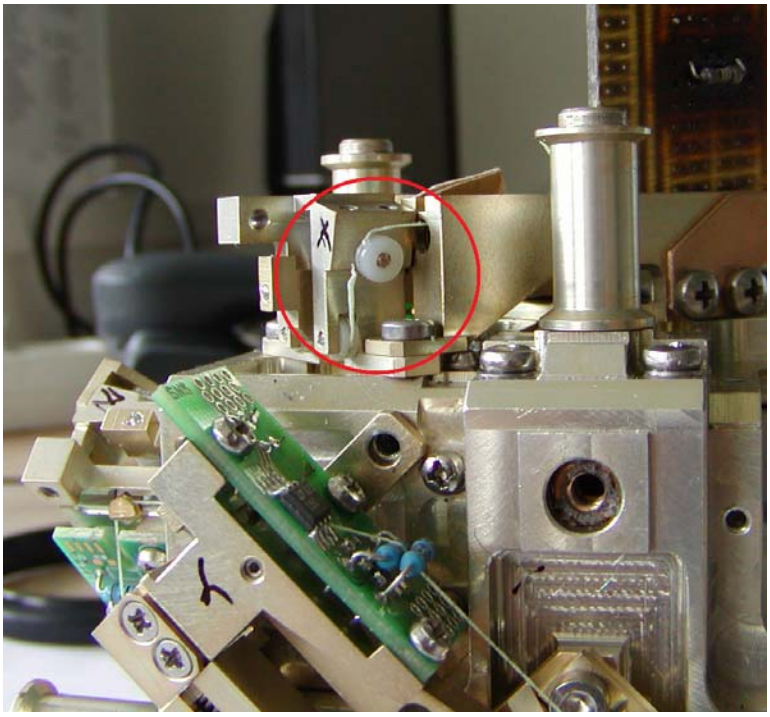

Figure 12 - Fiber was broken during some test

To better understand the LM behavior during vibration and to verify LM models an accelerometer was placed on the Lever above the slot with head of Locking Rod during vibration test (see Fig. 13)

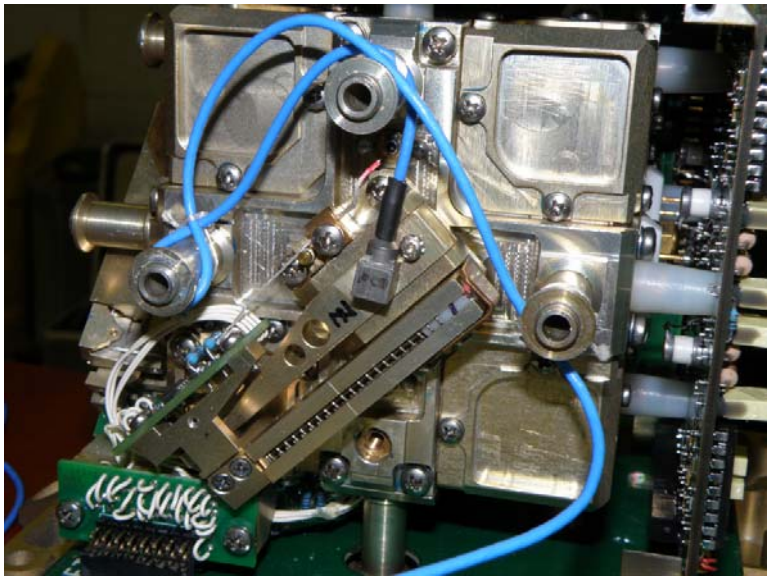

Figure 13 - Accelerometer on the Lever of z-axis LM

Qualification levels were applied in successive steps on all axes. No failure of fiber occurred any more. Responses in all three axis from random vibration (blue curve is spectrum applied in z-axis) on lever arm of LM locking z-axis are in the following Fig. 14.

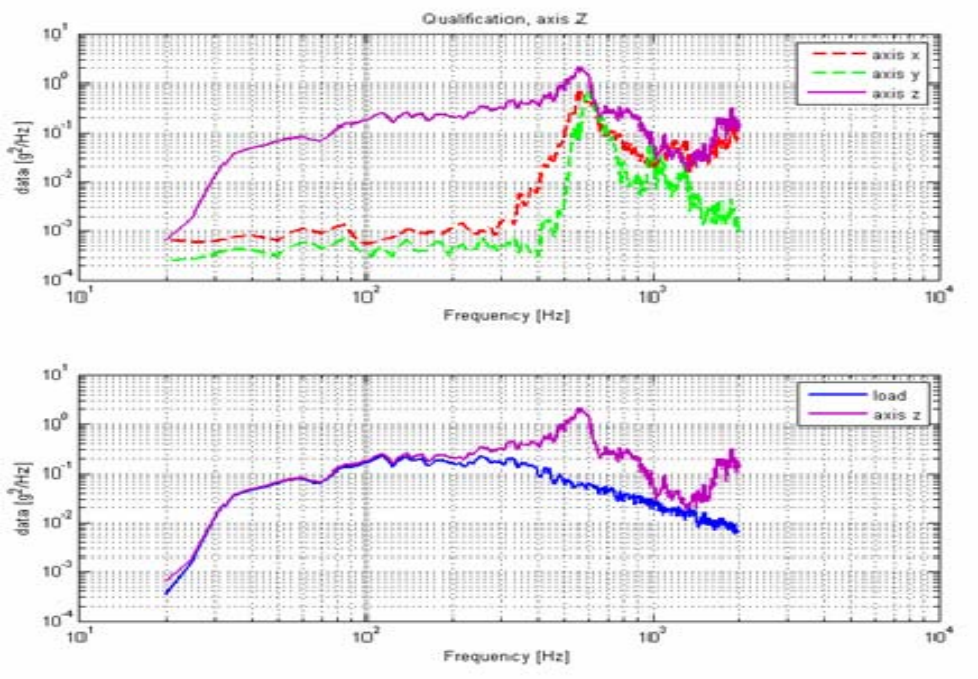

Figure 14 - Signal from random analysis

Conclusion

Locking mechanism (LM) of Microaccelerometer (MAC) was successfully redesigned. Set of qualification tests were carried out without any failure of LM.. Models in Matlab and in MSC.Adams predicted no loss of locking force during vibration test which is extremely important in order to cause no damage of Sensor. Above all model in Abaqus was created to analyze the behavior of fiber. It provided with important mechanical parameters for a new fiber with respect to load to be applied.

Nevertheless dynamic analysis performing with simplified virtual models did not involve every physical issue. Breaking fiber over sharp edges could not have been predicted neither from current model. The accuracy of model could also be refined to obtain lower differences in resonance frequencies.

Kinetics of the Thermal and Thermo-Oxidative Degradation of Polyethylene applied to Hybrid Rocket Motors

Susane Ribeiro Gomes[1], Leopoldo Rocco Jr[2], Koshun Iha[3] and José Atílio Fritz Fidel Rocco[4], ITA – Instituto Tecnológico de Aeronáutica, São José dos Campos, Brasil

The present research intends to explore the combined processes of the solid fuel condensed phase degradation and ablation, under the influence of the diffusion limited flame between gaseous oxidizer and fuel pyrolysis gases. The fuel condensed phase degradation has been considered one of the dominant parameters influencing combustion processes during hybrid rocket motors operation. In this investigation, samples of HDPE fuel grains have been studied in both inert (nitrogen) and synthetic air atmosphere by using thermogravimetry (TG) and differential scanning calorimetry (DSC) alongside with firing tests in labscale hybrid rocket prototypes. The kinetics parameters were determined by the isoconversional dynamic method based on TG and DSC curves with the use of several heating rates, the activation energy of thermal decomposition of the fuel was approximately 200 KJ/mol and this process started around 430° C. The kinetic study provided data for pyrolisis regression values. Simultaneously, labscale motor configurations were fired and the regression rate data was collected for each specified oxidizer mass flux. The temperatures and pressures were measures during the firing tests. Finally, based on pyrolysis regression rates and the combustion regression rate a mechanism for the polymer combustion process is proposed.

Introduction

It is of general awareness that hybrid rocket engines offer an attractive option to the risks and disadvantages associated with the solid and liquid engines (Altman, 2001). This alternative is a result of the increased security, reliability, ease of storage, oxidizer flow control valve and lower production costs typical of hybrid motors.

---

[1] Aeronautical engineer and master's candidate from Aeronautical Institute of Technology, ITA. First author.

[2] Mechanical engineer and PhD's candidate from Aeronautical Institute of Technology, ITA.

[3] Professor of Chemistry in Aeronautical Institute of Technology, ITA.

[4] Professor of Chemistry in Aeronautical Institute of Technology, ITA.

On the other hand, hybrid engines have inherent performance problems such as low density specific impulse, poor combustion efficiency and reduced mass fraction (Sutton and Biblarz, 2001). Additionally, the regression rate values, thus the total mass flow and total thrust, are below the values for the solid motors of similar size.

Therefore, the aim of this research is to improve the understanding of the underlying phenomena taking place in the diffusion limited flame. Hence, the factors involved in the combustion will be analyzed via two separate methods. The thermal analysis will provide comprehension about the solid fuel condensed phase degradation, and the firing tests in a hybrid rocket prototype will make available quantitative data about the real in depth characteristics of the burn on its operating conditions. The results will be then analyzed together and separately in order to find potential relationships between the two co-dependent phenomena.

Introduction to the thermal analysis

Renowned authors, (Ozawa, Isozaki, Negish, 1970; Flynn, 1966), demonstrated that differential scanning calorimetry (DSC) technique, based on the linear relationship between peak temperatures and heating rates, can be utilized to determine the kinetics parameters of thermal decompositions. The Ozawa method, also called isoconversional method, is one of the most recognized methods for estimating activation energies by means of linear heating rate experimental results.

Although the thermal analysis cannot be used to elucidate the complete mechanisms of thermal degradations, it provides reliable information regarding the dynamic analysis, namely the frequency factor, activation energy and overall reaction order calculations (Park, Lee, Kim and Yoo, 2000).

Kinetic Approach

The method used in the analysis of HDPE samples was based on DSC experiments. The temperatures of the extrapolated onset of the thermal decomposition process and the temperatures of maximum heat flow were determined from the resulting measured curves for exothermic reactions.

In order to determine the kinetic parameters of the degradation step Ozawa's method was applied. This method was derived from the basic kinetic equations of heterogeneous chemical reactions and therefore has a wide application, mainly since there is no requirement of knowing the reaction order (Ozawa, 2001) or the conversional function. The activation energy is the summation of activation energies of chemical reactions and physical processes occurring in the thermal decomposition and, for that reason, it is labeled apparent.

Presupposing that the constant rate follows the Arrhenius law and the exothermic reaction can be considered as a single step process, the conversion at the maximum conversion rate is invariant with the heating rate when this is linear. Thus carrying

out several experiments at different heating rates plots of $ln(\beta)$ vs $d(1/T_p)$ are prepared and the activation energy can be estimated directly from the curve slope using the following Eq. 1:

$$E = R\frac{d\left(ln\left(\frac{\beta}{T_p^2}\right)\right)}{d\left(\frac{1}{T_p}\right)} \quad (1)$$

Once time E is known the values of pre-exponential factor, A, are calculated with the Eq. 2:

$$A = \frac{\beta E e^{-E/RT_p}}{RT_p^2} \quad (2)$$

The temperature dependence between the specific rate constant k is described by the Arrhenius equation:

$$k = Ae^{-\frac{E}{RT_p}} \quad (3)$$

The kinetic Shimadzu software, based on the Ozawa method, collects the exothermic peak temperatures and the heating rate data and provides the Arrhenius kinetic parameters (E, A) related to the thermal decomposition of HDPE and, consequently, with the Eq. (3) the overall rate constant can be calculated.

Introduction to the labscale motor experiments

Experiments were conducted to ensure that our designs for hybrid rocket prototypes do work and can be utilized for the regression rate measurements. These firings took place on a test platform planned specifically for the tests of the labscale motors designed. Another purpose of the test was to ensure that the data acquirement and analysis was working properly.

Once the experiments validation was made, the set of labscale designs was tested with the purpose of investigating the flame behavior, combustion efficiency and principally the regression rates.

The length of the assembled chambers prior to combustion is 25 cm, and this value is based on the test bench facility available for this study. Two auxiliary chambers were set up ahead and aft of the grain. The pre-combustion chamber provides an uniform entrance condition with the effort of increasing the overall regression rates, while the post-combustion chamber provides better mixing of the gasifying propellants (Altman and Humble, 2001; Sutton and Biblarz, 2001).

The burning duration time of the single cylindrical grain ports of High Density Polyethylene was defined as 10 seconds, which was decided by a compromise

between the survivability of the nozzle without cooling and the time required for steady-state equilibrium to be successfully recorded.

Results Description

DSC curves were obtained on a model DSC50 Shimadzu in the temperature range of 298-1000 K, under dynamic synthetic air atmosphere (ca. 50 mL/min). Sample masses were about 20 mg, and each sample was heated in hermetically sealed aluminum pans. Four different heating rates were used for the HDPE samples: 20.0, 30.0, 35.0, 40.0 K min^{-1}. DSC system was calibrated with indium (m.p.= 429.6 K; ΔHfus=28.54 Jg^{-1}) and zinc (m.p.= 692.6 K).

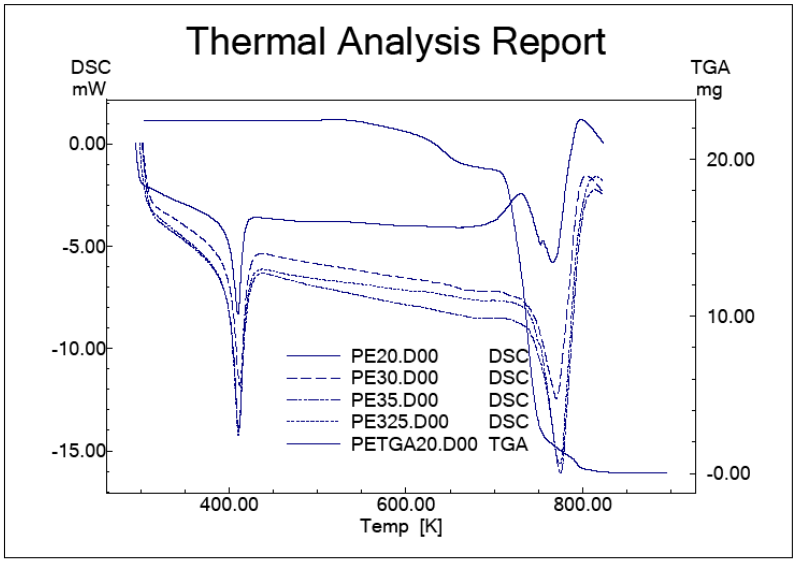

Figure 1 - DSC curves of thermal decomposition of HDPE samples, at the heating rates: 20, 30, 35 and 40 K min^{-1} and TG curve with a heating rate of 20 K min^{-1}

The activation energy and kinetic parameters of thermal decomposition of HDPE samples were calculated by Ozawa method using DSC curves at different heating rates: 20.0, 30.0, 35.0, 40.0 K min^{-1}. The activation energy of thermal decomposition of the fuel was approximately 200 KJ/mol and this process started around 430° C.

The firing tests produced an incredible amount of information about the combustion effects. The analysis in conjunction with the tangential velocities of the oxidizer injection methods produced considerable data to enlighten the comprehension of the mechanisms behind the blocking effects. The fuel grains profiles, Figures 2, 3 and 4, after burn show visible signs of the oxidizer flow pattern in accordance with the injection characteristics. The numerical results sustain the hypothesis that depending on the oxidizer flow tangential velocities the heat transfer increases, augmenting, therefore, the regression rates, even though more fuel is pyrolysed.

Figure 2 - Swirl oxidizer injector, model 1

Figure 3 - Axial oxidizer injector

Figure 4 - Swirl oxidizer injector, model 2

Conclusion

The Ozawa method demonstrated that differential scanning calorimetry technique, based on the linear relation between peak temperature and heating rate, can be used to determine the kinetics parameters of thermal decomposition reaction of HDPE giving reproducible results.

The DSC curves do not show any interference and the kinetic data obtained using the maximum temperatures (reciprocal, in K^{-1}) and the respective heating rates are very close to the results found in the literature, at very lower heating rates (Du, 1989; Rocco and co-workers, 2004; Andrade and co-workers, 2008; Andrade, Iha, Rocco and Bezerra, 2007).

The qualitative and quantitative analyses succeed on demonstrating all the hypothesis assumed on the works of Legenllč, Marxman and co-workers and bring further discussions about the mechanisms underlying the behavior of pyrolysed combustion gases in the boundary layer. A full paper study will describe the main correlations between the fuel pyrolysis regression and the fuel combustion regression rates.

Acknowledgements

The authors gratefully appreciate the financial support from CNPq (Conselho Nacional de Desenvolvimento Científico e Tecnológico).

References

[1] Altman, D., Holzman, A. (2007), *"Overview and History of Hybrid Rocket Propulsion."* In Chiaverini, M. J. and Kuo K. K. (Ed.), Fundamentals of Hybrid Rocket Combustion and Propulsion, American Institute of Aeronautics and Astronautics, Inc., Reston, Virginia, pp.1-36.

[2] Altman, D., Humble, R. (1995). *"Hybrid rocket propulsion systems,"* In Humble, R., Henry, G., Larson, W. (Ed.), Space Propulsion Analysis and Design, McGraw-Hill, New York, pp. 365–441.

[3] Andrade, J., Frutuoso, A. G., Iha, K., Rocco, J. A. F. F., Bezerra, E. M., Matos, J. R. and Suárez-Iha, M. E. V. 2008, *"Estudo da decomposição térmica de propelente sólido compósito de baixa emissão de fumaça"*, Quim. Nova, Vol. 31, No. 2, pp. 301-305.

[4] Andrade, J., Iha, K., Rocco, J. A. F. F., Bezerra, E. M. 2007, *"Análise térmica aplicada ao estudo de materiais energéticos"*, Quim. Nova, Vol. 30, No. 4, pp. 952, 956.

[5] Carmicino, C., and Russo Sorge, A. (2007), *"Performance Comparison Between Two Different Injector Configurations in a Hybrid Rocket,"* Aerospace Science and Technology, Vol. 11, No. 1, pp. 61–67.

[6] Chiaverini, M. (2007), *"Overview Review of Solid-Fuel Regression Rate Behavior in Classical and Nonclassical Hybrid Rocket Motos"* In Chiaverini, M. J. and Kuo K. K. (Ed.), Fundamentals of Hybrid Rocket Combustion and Propulsion, American Institute of Aeronautics and Astronautics, Inc., Reston, Virginia, pp.37-125.

[7] Du, T. 1989, *"Thermal decomposition studies of solid propellant binder HTPB"*, Thermochim. Acta, Vol. 138, 1989, pp. 189.

[8] Flynn, J.H. 1966, *"A quick, direct method for the determination of activation energy from thermogravimetric data"*, Thermochim. Acta, Vol. 4, pp. 323.

[9] Lengellé, G., Fourest, B., Godon, J. C., and Guin, C., *"Condensed Phase Behavior and Ablation Rate of Fuels for Hybrid Propulsion,"* AIAA Paper 93-2413, June 1993.

[10] Marxman, G. A., and Wooldridge, C. E., *"Research on the Combustion Mechanism of Hybrid Rockets,"* Advances in Tactical Rocket Propulsion, 25th Meeting AGARD Combustion and Propulsion Panel, April 1965.

[11] Ozawa, T. 2001, *"Temperature control modes in thermal analysis"*, J. Therm. Anal. Cal., Vol. 64pp. 109, 126.

[12] Ozawa, T., Isozaki, H. and Negishi, A. 1970, *"A new type of quantitative differential analysis"*, Thermochimica Acta., Vol. 1, No. 6, pp. 545, 553.

[13] Park, J.W., Lee, H.P., Kim, H.T. and Yoo, K.O. 2000, *"A kinetic analysis of thermal degradation of polymers using a dynamic method"*, Polym. Degrad.Stabil., Vol. 67, pp. 535.

[14] Rocco, J. A. F. F, Lima, J. E. S., Frutuoso, A. G., Iha, K., Ionashiro, M., Matos, J. R. and Suárez-Iha, M. E. V. 2004, *"Thermal degradation of a composite solid propellant examined by DSC – Kinetic study"*, J. Therm. Anal. Cal., Vol. 75, pp. 551, 557.

[15] Sutton, G.P. and Biblarz, O. (2001), *Rocket Propulsion Elements*, 7th ed., John Wiley & Sons, Chap. 15.

Instrumental Complex and Methods of Physical-mechanical Properties of Materials in Micro-method of Kinetic Nano- and Microindentation

Alekhin Valentin Pavlovich, Professor, Moscow State Industrial University, Moscow, Russia

A complex of devices and the methods of mechanical properties of materials in micro-kinetic method of nano- and microindentation. Instrumental complex and the technique allows: to make tests on nano- and micro-hardness in the low and ultra low loads to study the properties of thin surface layers, films, coatings, separate phases, etc., to evaluate the elastic and relaxation properties of the material on the relative magnitude of elastic recovery of indentation depth; test materials with poor reflective surfaces, such as polymers, as well as materials that have very strong impression resizes after unloading (rubber, semiconductors, carbides, nitrides, etc.) to study the operational properties of finished parts of small dimensions (instrumentation, microelectronics). The instrument allows to obtain a set of complex charts, surpassing such informative diagrams tension σ-ε. The developed techniques and computer processing of diagrams indentation can also determine the following characteristics of the material [1-2] (Fig. 1):

- Young's modulus, yield stress and strength, uniform elongation;
- Hysteresis losses and damping properties of material;
- Strength and energy of adhesion of coatings - the two fundamental parameters;
- Such compositions;
- Study of performance properties of finished parts of small dimensions (instrumentation, microelectronics);
- Fracture toughness and effective surface energy;
- Structure of the material and the distribution of particle phase (or pores) in size and volume fraction;
- Dependence of mechanical properties on strain rate;
- Monitor and optimize high-end technologies in problem solving improve the reliability, durability, efficiency and capacity of different models of equipment.

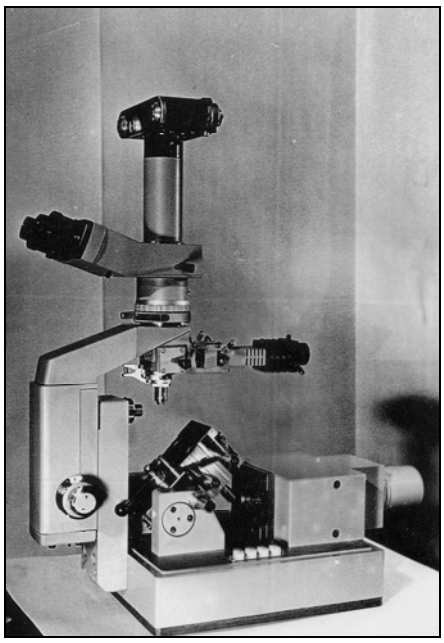

Fig. 1 - The appearance of the complex instrumentation UTM-12 for kinetic micro- and nanoindentation.

Introduction

At present, virtually the only method for measuring mechanical properties in micro is a method of measuring the microhardness, implemented on a standard device type PMT-3. However, the key moment is the fact that this method gives a very modest information - in fact, only the value of microhardness as average contact pressure on the material. The proposed method greatly expands the possibility of determining the mechanical properties of materials in nano-and micro-volumes. A typical diagram ”Load P - indentation depth h“, obtained by such a test, represented in Figure 2.

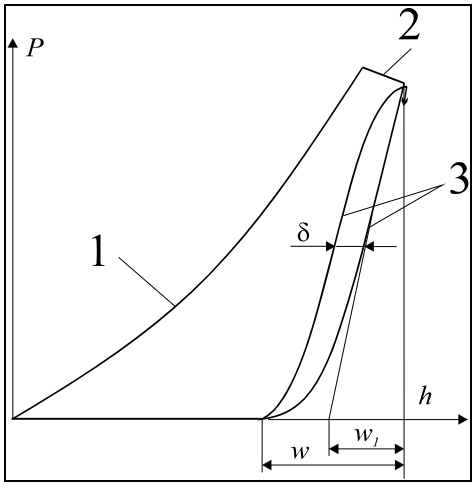

Fig. 2 - Figure indentation with three sections: 1 - loading 2 - under load, 3 - unloading and repeated loading

Her areas of 1-3 depend on three material properties: resistance Hh elastic-plastic deformations (1), creep or stress relaxation (2) and the elastic properties (3).

Hysteresis loop width δ is registered under repeated loading of the same fingerprint. It determines the intensity of accumulation of total local plastic deformation under cyclic loading, and consequently, affects the processes of wear and tear on the kinetics of crack growth in fatigue.

Figs. 3 - 4 show an illustration of the method when testing advanced materials and coatings:

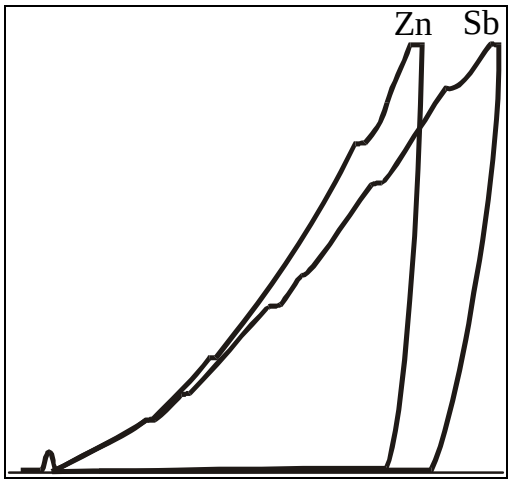

a)

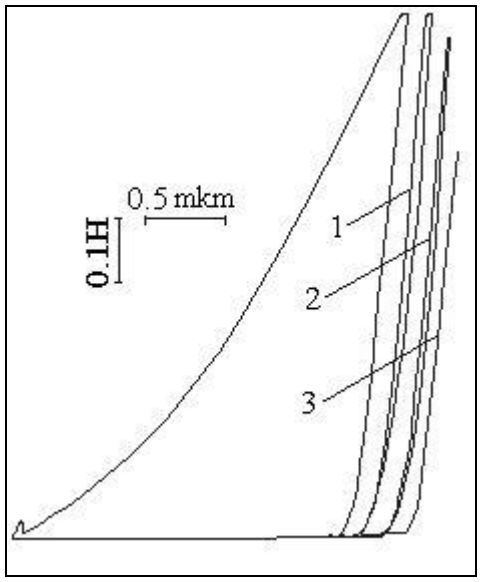

b)

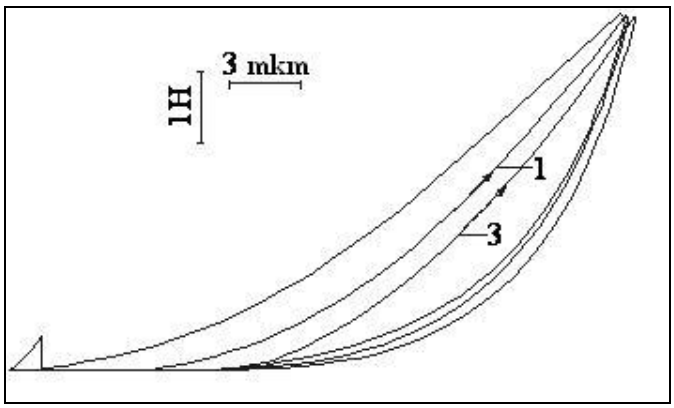

c)

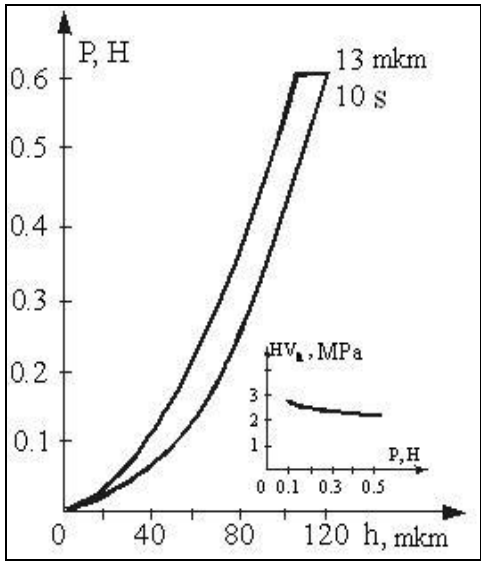

d)

Fig. 3. Some features of the indentation diagrams for various materials:

a) *- deformation twinning in zinc and antimony (the step on the branches of loading);*
b) *- the narrowing of the hysteresis loop on steel 30ХГСА in cycles 1-3 with a decrease in the load P / Pmax in repeated cycles: P / Pmax =: 1 - (1); 0,95 - (2), 0,8 - (3);*
c) *- the same for pyrography IPY-5 at P / Pmax = 1 (the imprint is visible under the microscope after about 10 cycles);*
d) *- one of the varieties of rubber: pronounced creep at maximum load and 100% recovery of depth on the unloaded imprint;*

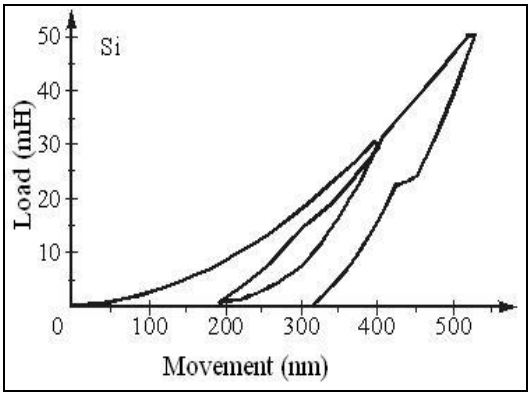

e)

e) - the anomalies in the hysteresis loop on silicon with nanoindentation (WC Oliver), caused a reversible phase transition of the material under the indenter: increased width of the hysteresis loop shifted to the load on the excesses of its branches. With the increase of the load appears on the branch unloading step (output subsurface brittle fracture surface.

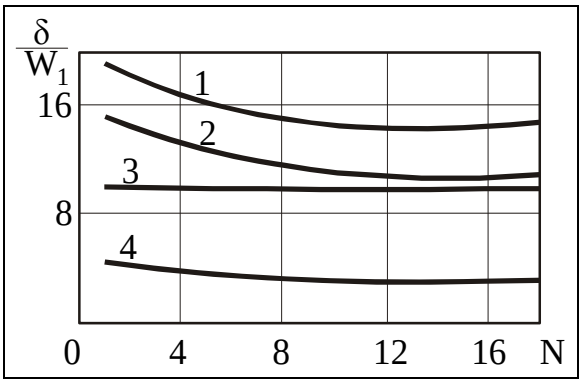

Fig. 4. - The dependence of the strain hysteresis δ/W_1 number N of repeated cycles of loading:

1, 2 - steel U8A and 30ХГСА 3 - Glass Industrial 4- Д16АТ. Deformation of crystalline materials to stabilize after 10 - 12 cycles of loading. Hysteresis on the glass does not depend on N and is similar to hysteresis that occurs during a reversible phase transition

Fig. 5 shows the histogram for the two-phase material consisting of the baseline equal volume fractions of Fe and Cu, obtained by traditional quantitative analysis:

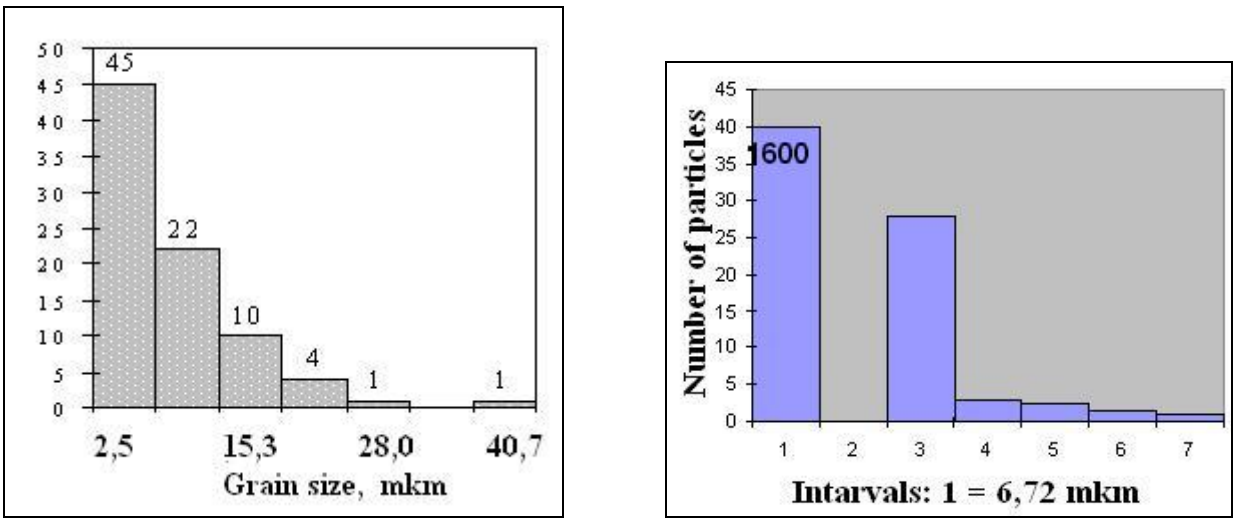

a) *b)*

Fig. 5 - Comparison of histograms obtained by the traditional quantitative analysis (a) and proposed for x = 3 [2] (the first interval contains 1600 particles Fe-Cu) (b)

Objective

Objective - development of methods for studying physical and mechanical properties of materials in micro-kinetic method of nano-and microindentation.

Main results

- Based on the analysis of elasticity problems the generalized Hooke's law for any case of elastic-plastic local contact loading, measured by the fact that the diagram vdalivaniya the slope of the initial part of a branch of unloading indentation hardness with minorities and the area A does not depend on the law of the distribution of average pressure on contact area. The expressions for Young's modulus on the angle with plastic indentation of the indenter, including material for thin coatings and microparticles, as well as to determine the stiffness of the measuring device.
- The relation between the reduced (traditional) H and nonreduced Hh hardness, depending on the normal elastic deformation of the contour of the impression and the height of the roller extruded material (bulk). The methods of determining the height pile basic mechanical characteristics of the material; this height is determined from the difference between the calculated and experimental ratio of reduced and nonreduced hardness.
- An analytical expression for calculating the value of the reversible plastic deformation in the imprint, which determines the kinetics of the exhaustion of

ductility in terms of wear and fatigue. It is shown that the indentation of the indenter, this deformation (hysteresis) consists of two components: the traditional strain Bauschinger and reverse plastic deformation associated with the local chamber of deformation on the dimensional level h. An analytical relationship between the true values of hysteresis, expressed through the plastic and elastic deformation in the imprint.

- Grounded kinetic parameters that determine the dependence of hardness on strain rate: the rate of penetration, the true strain rate during indentation, the activation volume. Show quantitative agreement on the order of magnitude estimates of the activation volume, obtained by indentation and uniaxial loading.
- Methods for estimating the porosity of materials, based on measuring the sealing of the plastic zone under the imprint under the influence of high hydrostatic pressure. Seal is fixed to reduce the height of pile, which is found from a comparison of the reconstruction and nonreduced hardness.
- Formulated and solved in a first approximation, a statistical problem of connection coefficient of variation and histograms of the microhardness of nano-structure of the material (Fig. 5). On this basis, proposed a new method of analyzing the structure. It is noted that in the case of analyzing the structure of monophasic materials and single crystals of the role of particle phase is transferred to the fragments of the structure arising at the appropriate level of plastic deformation in the imprint.
- Design of the device for testing the method of kinetic indentation reserved a number of copyright certificates and introduced a number of organizations.

Findings

The experimental diagram Ph kinetic microhardness method for determining Young's modulus, hysteresis loss, the porosity of materials. The relation between the reduced (traditional) and nonreduced hardness. Formulated and solved the problem of statistical relation coefficient of variation and histograms of the microhardness of nano-structure material.

This work was financially supported by a search of research work (project NK-556P (114)/3, the state contract № P545) as part of the Federal Program *"Scientific and scientific-pedagogical cadres Innovative Russia"* in the years 2009-2013.

References

[1] Bulychev SI, Alekhin VP.: *Material testing continuous indentation of the indenter*; Moscow, Mashinostroenie, 1990

[2] Bulychev SI.: *Basic kinetic nano-, micro-and macroindentation: monograph*; Moscow, Moscow State Industrial University, 2008

Photon Counting Detectors for Laser Ranging and Laser Time Transfer Missions

Ivan Procházka, Josef Blažej, Czech Technical University in Prague, Czech Republic

We are reporting on research, development, and operational results of the photon counting detectors that are being developed in our lab for ground laser ranging and space missions related to laser ranging or precise time transfer by laser pulses. The detector is based on silicon avalanche photodiode operated in a special mode with single photon detection capability in optical wavelength region. The detection chip our provenience is controlled by a dedicated circuit. The circuit allows biasing and active quenching of detection structure. The bias is controlled by optional external gate. The ground version of detector is optimized for an precision time tagging of an incoming laser pulse in order of several picoseconds. The space versions of detectors are optimized for an on-board detection and precision time tagging of an incoming laser pulse.

Satellite laser ranging

Over fifty years ago, the invention of the laser revolutionized the way we live. One of the most phenomenal and useful data producing application of laser in applied physics is the satellite laser ranging (SLR) – a technique to measure the distance between Earth and artificial satellite of Earth using very short laser pulses and fast single photon sensitive optical detector. The launching of specialized geodetic artificial satellites (1964) with corner cube retro-reflectors enabled the laser distance measurement in space scale.

The principle of SLR is similar to radar, but working with optical signal. Short (in beginning 10^{-8}, now 10^{-11} s) laser pulse is transmitted in well defined time (measured from optical laser output) to the satellite (it is necessary to track it), reflected back to receiving telescope and detected by a single photon sensitive detector with high (10^{-9} – 10^{-11} s) temporal resolution. The result is time of measurement (called epoch) from independent clocks synchronized with UTC and time of flight of laser signal measured by precise time interval meter. To manage high repetition rate of experiment all main subsystems have to be controlled electronically. From knowledge of time of flight and local meteorological conditions, the accurate distance between station and the satellite can be calculated applying known atmosphere models. Ranging data are sent to international data centers for accurate satellite trajectory calculation using data from many SLR stations. This is why the SLR technique is inherently international.

The first successful experiments were announced in USA, where this problem was solved on several institutions (1967–69). The second country was France (1969). And the third country was Czechoslovakia (1970) on Ondrejov observatory. Three institutes have directly cooperated together: Faculty of Nuclear Sciences and Physical Engineering of Czech Technical University in Prague (Karel Hamal as project leader), Astronomical Institute of Czechoslovak Academy of Sciences, and Research Institute of Geodesy in Prague. During years 1970-1990 the Czechoslovak team operates as a system integrator and the network of SLR stations was build and operated in several countries (Egypt, Bolivia, Poland, India, Cuba, Ecuador, USSR, Bulgaria, VietNam). The most of necessary subsystems can be covered by a local production (e.g. our department was producing the lasers for all mentioned stations [1]) with only one exception – the photomultiplier (PMT). To eliminate the dependency on import of expensive devices the research on field of all-solid-state semiconductor single photon counter was initiated. The first samples with acceptable properties were completed in 1984.

Single photon avalanche detector

The overall idea of this type of detector was not new. The avalanche photodiodes acting as photon counting devices has been pioneered by Cova and co-workers [2]. This detector, called Single Photon Avalanche Diode (SPAD), is an avalanche photodiode structure prepared using a conventional planar technology on silicon reported by Haitz [3]. Single photon sensitivity is achieved by biasing the diode above the junction breakdown voltage. In this stage the first absorbed photon is capable of triggering the avalanche multiplication of carriers; a fast rise-time current pulse is generated. The leading edge of the current pulse marks the event of the photon absorption with picosecond accuracy. The current increase is terminated by an external circuit connected to the diode, where the typical value of the gain achieved exceeds 1×10^9. Such an operation mode is called a Geiger mode. The operation of the detector may be controlled: gated, by an external electrical signal. The detector is activated short time before the arrival of the photon of interest. As the our SPAD technology was developed really independently from above mentioned groups and in fact as a spin-off of silicon neutron detectors, the resulting structure is similar, but in principle different. The biggest drawback is its bigger darkcount rate, but it is acceptable for application such as SLR, because inherent background signal is even high. The biggest positive difference is the higher radiation hardness allowing operation on orbit with acceptable shielding [4].

Laser time transfer

Ten years ago the extension of SLR technique was proposed – laser time transfer. The goal of any time transfer mission is to measure the difference ΔT between clock signal on ground and on board, see Fig. 1. The standard satellite laser ranging with

passive reflection from satellite is extended by active optical signal time-tagging on board. This is a place to exploit the radiation hardness, low operation voltage and low weight of SPAD. All running and planned time transfer missions are using the existing ground segment – well established network of satellite laser ranging stations. In compare with microwave link it allows principle decreasing of systematic errors from nanosecond to picosecond range due to shorter wavelength and better signal propagation prediction through atmosphere. It is relatively easy to implement on-board. The biggest drawback is that clean sky necessary, laser time transfer is not suitable for routine operation, it is technique for time to time independent system calibration.

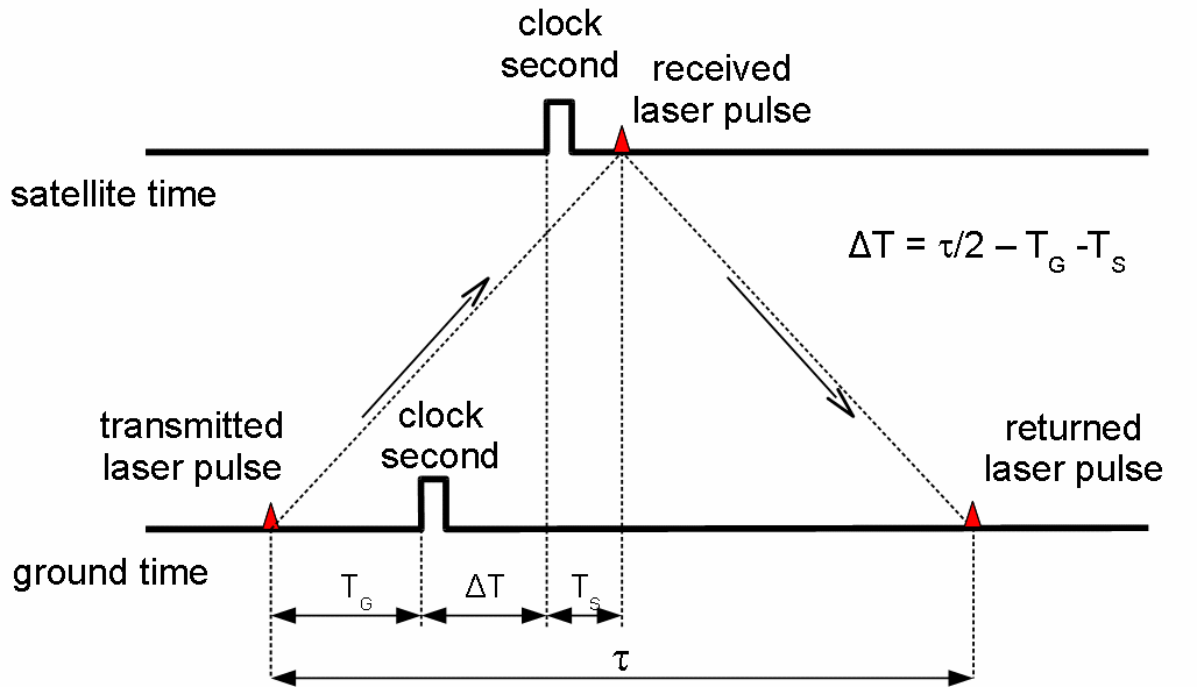

Figure 1 - The principle of laser time transfer

Space-oriented applications

Together with SLR application the unique properties of SPAD was used in following space projects. The first was USSR mission Mars 92. A part of planned mission was a heliostat, a balloon flying near to Mars surface (0–1 km). The SPAD was used as a detector of single photon counting altimeter developed in cooperation with IKI Moscow. Mission was postponed to 1996 and crashed during start phase. The analogical device succeeds in NASA tender to scientific payload of Mars Polar Lander 98. It was low weight (940 g), low consumption (4 W) single photon LIDAR constructed in cooperation with IKI Moscow. It was projected for two operation modes, 0–700 m DIAL for low cloudiness analysis, and 1–10 km for high cloudiness registration. The mission crashed during landing due to navigator fault.

The third mission has been completed. The Laser Time Transfer (LTT) instrumentation has been launched on board of the Chinese experimental navigation satellite Compass-M1 to a high altitude orbit of 21500 kilometers, launch, April 13 2007, 20:11 UTC. Beidou (Chinese analogy of Ursa Major) is a project to develop an independent Chinese satellite navigation system, see Fig. 2. Its successor is called Beidou-2 or Compass. Since half of 2008 it produces results from LTT experiment, data precision and overall data yield are limited by downlink data capacity and by a specific mistake in field of view of detector [5]. The single shot precision is about 300 ps. The next LTT payload for the next Compass mission with bigger downlink capacity is planned by the end 2010. The fourth mission is Time Transfer by Laser Light (T^2L^2) module at France – USA mission Jason–2, launched June 20 2008. T^2L^2 is a complex experiment providing realtime signal strength monitoring by a linear photodetector. This information is used for compensation of precise timing providing by SPAD. Since 2009 it is producing data, again limited by experimental character of satellite. The interpretation of single shot precision is more complicated due to complexity of entire experiment including data processing on-board.

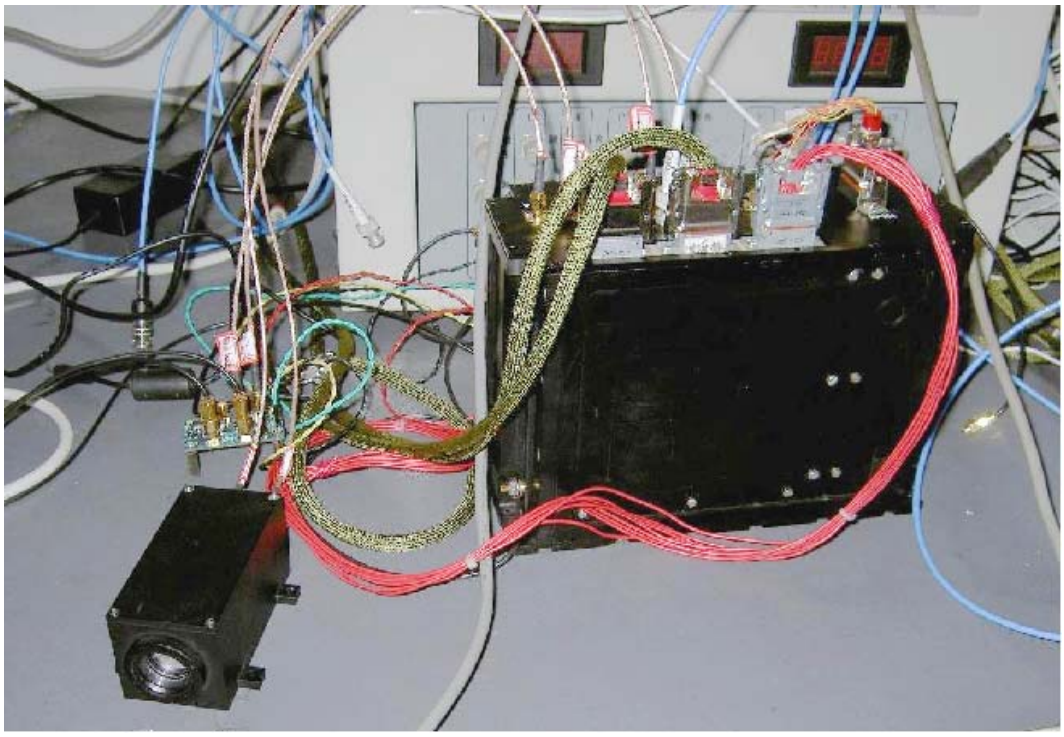

Figure 2 - Chinese LTT flight unit laboratory test, small black unit (left) – optics and electronics, SPAD inside, bigger black unit (right) – power and timing unit, power source and test bench in background

Currently, the European laser time transfer (ELT) at Atomic Clock Ensemble in Space (ACES) is under development [6]. The ACES is scheduled to launch in 2013 to International Space Station, module Columbus. The designed single shot precision is 50 picoseconds. ESA prime contractor for ELT module development is Czech Space Research Centre, Inc.

Indoor calibration and demonstrators

The necessary condition for successful laser ranging, LIDAR, altimetry, and time transfer instrument development and testing is well-equipped laboratory providing picosecond laser sources, reference detectors with high temporal resolution, optical bench for indoor laser radar demonstration, and precise and stable timing electronics that allows measure instrument parameters in time scales comparable with entire orbit. Our laboratory fulfills all listed requirements including unique time interval meter with 4 femtosecond stability [7]. The complex optical part and electronics demonstrators were developed in cooperation with IKI Moscow and DLR, currently the new one demonstrator is developed in cooperation with Aeronautical research and test institute, Prague.

References:

[1] Hamal K. - Jelinkova H.: *Compact satellite ranging laser subsystem*; IEEE Journal of Quantum Electronics, Vol. 14, No. 10, p. 701, 1978

[2] Cova S. - et al.: Journal of Modern Optics 51 (9-10), 1267-1288, 2004

[3] Haitz R. H., Journal of Applied Physics 35, 1370, 1964

[4] Procházka I. - Hamal K. - Sopko B.: *Recent Achievements in Single Photon Detectors and Their Applications*; Journal of Modern Optics, Vol. 51, No. 9-10, p. 1289-1313, 2004

[5] Procházka I. - Sopko B. - Blažej J.: *Single-photon detector operating under extremely high background photon flux conditions*; NIM-A. 2009, Vol. 610, No. 1, p. 342-344

[6] Procházka I. - Schreiber U. - Schäfer W.: *Laser time transfer and its application in the Galileo program*; Advances in Space Research. accept. for publ. 2010

[7] Pánek P. - Procházka I. - Kodet J.: *Time measurement device with four femtosecond stability*; Metrologia 47, 1-4, 2010

Remote Sensing Center at a University for Real-time Acquisition of High Resolution Optical and Radar Imagery

Vladimir Gershenzon[a], Olga Gershenzon[b], Marina Sergeeva[c], Vitaly Ippolitov[d]

[a]General Director, R&D Center ScanEx, Moscow, Russia
[b]Vice-president, R&D Center ScanEx, Moscow, Russia
[c]Deputy General Director, R&D Center ScanEx, Moscow, Russia
[d]Head of Department, R&D Center ScanEx , Moscow, Russia

The task of increasing the economic competitiveness of any country is not possible without reinforcing the role of the higher professional education. Today, the traditional education, as an access to learning, can not keep up with the current requirements of science and industry.

Russian company R&D Center SCANEX proves on a practice that setting up Remote Sensing Centers allowing real-time imagery acquisition from Earth observing satellites within the structure of Universities is one of the solutions of the above mentioned problems. This will provide the proper environment for innovative education, to deliver the efficient training for scientific and academic and teaching personnel, secure the role of the young professionals in science, education and hi-tech, and maintain the continuity of generations in science and education. SCANEX has delivered the land based UniScan™ centers to over 20 higher education institutions in Russia, Kazakhstan, and Spain. These stations serve as the basis for Earth monitoring from space centers providing the training and advanced training to produce the specialists having the state-of-the-art knowledge in Earth Remote Sensing and GIS, as well as the land-use monitoring and geo-data service for the economic operators in such diverse areas as the nature resource management, agriculture, land property management, etc.

Since year 2009 satellite imagery service to Universities has extended worldwide outside the Russian territory, providing EROS A satellite imagery at 1.8 m resolution, IRS-1D imagery at 5.8 and 23 m, SPOT 4 satellite imagery at 10 and 20 m resolution, and SAR RADARSAT-1 imagery with resolution ranging from 100 m to 8 m. Based on the Agreement between SCANEX and the satellites Operators, and on unique flexible financial terms, the international universities can purchase the universal compact UniScan™ stations including telemetry for the first year of operation. Creation of state-of-the-art remote sensing centers at universities will lead to a new quality level for education and scientific studies and will enable to make education system in such innovation institutions open to modern research work and economy.

Introduction

The task of increasing the economic competitiveness of any country is not possible without reinforcing the role of the higher professional education, attracting youths to deliberate choice of future profession. Today, the traditional education, as an access to learning, can not keep up with the current requirements of science and industry.

Such an index as the education quality comes along with education results, currently most often referred to as “competence”. Innovation of education should be more competence-oriented than passing of knowledge that always gets out of date. Following this pattern knowledge can be acquired on an individual bases. Such kind of education should be more connected to practice than the traditional one.

Reducing competitiveness of traditional education institutions, as well as insufficient science and production integration indicate that new types of higher education institutions should be established. Nowadays, often traditional education as the system of gaining knowledge lags behind the actual current requirements of noc-temporary science and production.

Solution from ScanEx

One of the solutions to resolve these problems can be the introduction of Remote Sensing Centers for Earth observation from Space for territories changes monitoring as research and development links in the chain of universities. This will allow the students to master practical skills having an ultra-modern laboratory base.

Traditionally remote sensing centers at universities are equipped with ground stations enabling to receive free data, such as worldwide known AVHRR from NOAA satellites series with resolution of 1,100 m and MODIS from Terra and Aqua satellites with 250, 500 and 1,000 m resolution. Important positive peculiarity of these data in that there are many open and free software tools and many of them can be found in Internet. This opens a wide field for students and researchers to change of knowledge, ideas and new developments investigating AVHRR and MODIS data for global changes on vast territories. But low resolution of these data makes considerable restrictions for their practical applications for more precision changes of local areas of the Earth.

At the same time one who wishes to receive data with middle and high resolution faces with such problems as high price for ground station and expensive telemetry fee. Usually only national large remote sensing centers have a possibility to receive data with middle and high resolution, both optical and radar. However, it was a dream for universities...

Since 2009 ScanEx provides the possibility of equipping universities all over the world with technologies for receiving Earth remote sensing data of high resolution (up to 1.8 m) in real time. Participants of the world educational community can purchase the universal UniScan™ ground station for receiving Earth observing data

already completed with licenses for the right to receive 100 scenes of EROS A, 600 minutes of IRS-1D, unlimited access to SPOT 4 images and 50 scenes of RADARSAT-1 for the first year of operation. Initial inclusion of the license in the functionality of UniScan™ ground station (pursuant to agreements with the Operators of respective Earth remote sensing missions) leads to significant cost reduction of receiving station and space imagery for universities. As a result the world universities will be able to effectively utilize the state-of-the-art space technologies in their educational process and scientific research by working with up-to-date satellite data received at their own stations with the footprint of up to 2.5 thousand kilometers in radius.

Experience and technology

To date, there are over 20 Remote Sensing Centers/Laboratories operating on UniScan™ ground stations deployed at the leading universities in Russia, Kazakhstan and Spain. In the most cases they receive MODIS data. But among them 7 UniScan™ ground stations in universities of Russia are equipped not only for MODIS data, but also for other satellites (SPOT 4, IRS-P5, IRS-P6, EROS A/B, RADARSAT-1) thanks to flexible licensing policy implemented in the Russian Federation.

Based on SCANEX technology Remote Sensing Centers have already been operating with an excellent track record in such Russian Universities as Altay State University, Belgorod State University, Ufa State Aviation Technical University, Tyumen State University, Moscow State Technical University n.a. N.E. Bauman.

Samara Space Geoinformation Center has been operating in Samara State Aerospace University since December 2006, and is currently the best equipped Earth Remote Sensing Center in Russia and CIS countries, not only among the educational facilities, but also the state and private space monitoring centers.

Earth Remote Sensing Centers have been launched in 2007-2008 as a part of “Education” National Project in Siberian and Southern Federal Universities.

It has been currently the worldwide practice to set up Remote Sensing Centers at the higher education entities and other educational organizations. Thus, UniScan™ based laboratories and centers have been in operation at Kazakhstan-British Technical University of Republic of Kazakhstan (Almaty) under the auspices of Kazakhstan System Modeling Research Institute, at Satpayev Kazakhstan Research Science and Technology Institute (Almaty), at two universities in Spain (Valladolid and Valencia).

The Remote Sensing Centers deliver the real-time training for executive decision making support technology at the regional and municipal levels. The Centers can also provide the commercial service as well, e.g., training at professional development programs, contracted areal monitoring work management in a range of various applications (management of natural resources, agriculture and forestry management, emergency response, mapping updates, cadastral work, etc.) or research and development in various fields of knowledge.

UniScan™ ground station is intended for receiving and processing information transmitted from Earth low-orbit satellites via X-band radio channels with the data rates up to 170 Mbps in one channel. Such rates correspond to images with a spatial resolution better than 1 meter. At present the UniScan™ station provides for reception and processing of data from Terra, Aqua, IRS-P5, IRS-P6, CARTOSAT-2, SPOT 4/5, FORMOSAT-2, EROS A, EROS B and RADARSAT-1/2, ENVISAT-1 satellites.

UniScan™ hardware is universal and programmable and, in most cases, ground station can be upgraded for new satellites on the software level.

UniScan™ is completed with software for data reception, preliminary processing, archiving, cataloguing and creation of thematic products further to be imported into various GIS formats and applications. The most popular among the specialists in Remote Sensing and GIS are ScanMagic® and ScanEx Image Processor® software applications with more than 200 licenses throughout Russia and abroad.

Fig. 1. - UniScan™ ground station at the University of Valencia, Spain

Remotely sensed data application

Data received from the satellites in real-time are converted into ready-for-further-analysis products within 0.5-1 hour after being received from space, which indicates a high operational degree of the process (no data, available via Internet, can be obtained in such a quick mode).

Remotely sensed data received by Remote Sensing Center of an university will allow resolving following practical tasks concerning change detection using different types of remotely sensed data both optical and radar:

- topographic maps updating;
- forest fires early detection and monitoring;
- ice and snow cover condition operational assessment;
- on/off shore oil spills detection within the oil production and transportation areas;
- ships detection in the seas;
- ecological situation of water areas and new seaports, pipelines and oil terminals construction sites;
- illegal fishing control;
- license agreements compliance monitoring within the fields of natural resources development;
- forestry monitoring (logging dynamics, logging status);
- agricultural monitoring for crop rotation rules observation and proper arable lands use;
- illegal construction control;
- monitoring of infrastructure development;
- independent and operational natural disaster damage assessment;
- hydraulic structures condition monitoring;
- creation of up-to-date thematic maps of natural objects condition (vegetation, soil cover, areas hazard rate, etc.);
- environmental impact assessment of a territory development.
- solution of hydro-meteorological and weather forecast tasks;
- environmental monitoring and others.

Contemporary Remote Sensing Center at an university allows to:

- turn the university into one of the world leading education institutions equipped with cutting-edge technology and firmware for Earth observation from space (footprint of ground station is about 12 million square kilometers);
- carry out training and advance training of specialists having skills in remote sensing and GIS, used for decision-making support;
- monitor territories and submit data in support of decision-making of regions and sub-regions.

Summary

UniScan™ ground station technology developed by ScanEx and implemented for over 20 Remote Sensing Centers/Laboratories at universities enables new unique possibilities to receive in real-time high resolution optical and radar data on standard personal computer of users.

Since year 2009 satellite imagery service to Universities has extended worldwide outside the Russian territory, providing EROS A satellite imagery at 1.8 m resolution, IRS-1D imagery at 5.8 and 23 m, SPOT 4 satellite imagery at 10 and 20 m resolution, and SAR RADARSAT-1 imagery with resolution ranging from 100 m to 8 m. Based on the Agreement between SCANEX and the satellites Operators, and on unique flexible financial terms, the international universities can purchase the universal compact UniScan™ stations including telemetry for the first year of operation. This is the first precedent in the world.

Conclusion

Creation of state-of-the-art Remote Sensing Centers/Laboratories at universities will lead to a new quality level for education and scientific studies and will enable users to make educational system in such innovation institutions open to modern research work and economy.

Brno University of Technology: Space Activities of Research Establishments and Academia in Czech Republic

Jiří Hlinka, Miroslav Šplíchal, Institute of Aerospace Engineering, Brno University of Technology, Brno, Czech Republic

The paper describes past and current space related activities of Institute of Aerospace Engineering at Brno University of Technology. It also gives an overview of knowledge, skills and equipment available at the institute showing potential of Czech academic environment for wider cooperation in space activities. Activities of the Czech Aerospace Research Centre will also be presented. The centre involves top research organizations from whole Czech Republic with focus on aviation and space applications.

The paper will demonstrate opportunities for further cooperation of industrial and research partners with both, academia and research establishments in the Czech Republic.

1 Introduction

Starting participation of Czech Republic in ESA (European Space Agency) is a result of long time historical development on space field. Beginnings can be tracked down to 60's of the last century. Czechoslovakia at that time had well developed industry, especially aviation industry.

First significant project was design of suborbital meteorological rockets SONDA that took place in Czechoslovakia between 1965 and 1966. However, most of professional space activities were concentrated in Interkosmos programme. Czechoslovakia could be considered as one of most successful participants of the programme at that time. Czechoslovak devices were mounted on practically all Interkosmos scientific space probes. In 1978, Vladimir Remek became first cosmonaut that was not citizen of SSSR or USA (thanks to his participation in the mission of Soyuz 28). An important project (and successful) were also Magion space probes (1978-1996). Magion 1 was the first space probe build completely in Czechoslovakia. It was launched together with Interkosmos 18. Major mission objective of this couple of space probes was research of interactions between magnetosphere and ionosphere. In next 18 years, another 4 Magion space probes were launched into space. Besides own space projects, scientists and engineers from Czechoslovakia participated on development of different devices for space use. Most widely known is probably crystallizer CSK for Saljut and Mir space stations [6].

After the end of the Interkosmos programme (at beginning of 90's of last century) and after splitting of Czechoslovakia, space research in Czech Republic came to difficult position. Most of the research institutions were without academic and governmental support. Many teams finished their work, some tried to continue after privatization. However, significant knowledge and capacities still exist in Czech Republic and are recently growing.

The paper will present capacities, knowledge, skills and equipment available on one of significant academic facilities, Institute of Aerospace Engineering at Brno University of Technology. It should demonstrate opportunities for further cooperation with space oriented industrial partners.

2 Brno University of Technology / Institute of Aerospace Engineering

Brno University of Technology (BUT) is second biggest technical university in Czech Republic. Whole BUT consists of 8 faculties and has over 23 000 students. Topics covered by the university include wide spectra of technical and scientific disciplines, from mechanical engineering, electrical engineering and information technologies, through civil engineering and chemistry to architecture and arts.

Institute of Aerospace Engineering (IAE) is part of Faculty of Mechanical Engineering at BUT. IAE is primarily focused on education of young aerospace engineers and scientists. It provides education in three major areas: **Aircraft design** (master study), **Aeronautical traffic** (master study) and **Professional pilot** (bachelor study). Education in design specialization pays attention among others on following major branches:

Design and structural analyses

- design and stress analyses of lightweight structures made of modern aerospace materials. In particular, attention is put on structures from modern aluminum alloys and composite materials. IAE has significant experience with FE (Finite Element) modeling including material and geometrical nonlinearities. Long time experience includes close cooperation with top European industrial and research institutes, like EADS and DLR (for example within CEDESA or CELPACT projects).

Safety and reliability

- safety and reliability assessment of technical systems with attention on methods and procedures suitable for aerospace use. IAE also actively participated on practical reliability analyses done in accordance with ECSS standards – safety assessment of microaccelerometer for space use.

Materials

- properties of advanced metal and composite materials for aerospace use (including for example GLARE) are subject of research and testing at IAE. The equipment includes wide variety of testing equipment and additional equipment, i.e. owens, autoclave, etc.
  Since 2011, IAE will also have own clean room for material research (non-space certif.).

Testing

- although IAE's certified testing lab (with approval for testing of aviation structures from Civil Aviation Authority) is primarily focused on testing of aircraft structures and no clean room is available directly at IAE, it possible to use wide variety of testing equipment to perform structural tests of mock-ups and ground jigs. Also, additional measurement and documentation equipment can be used – for example high speed camera, endoscope, eddy currents testing equipment (Foerster Defectometer), etc.

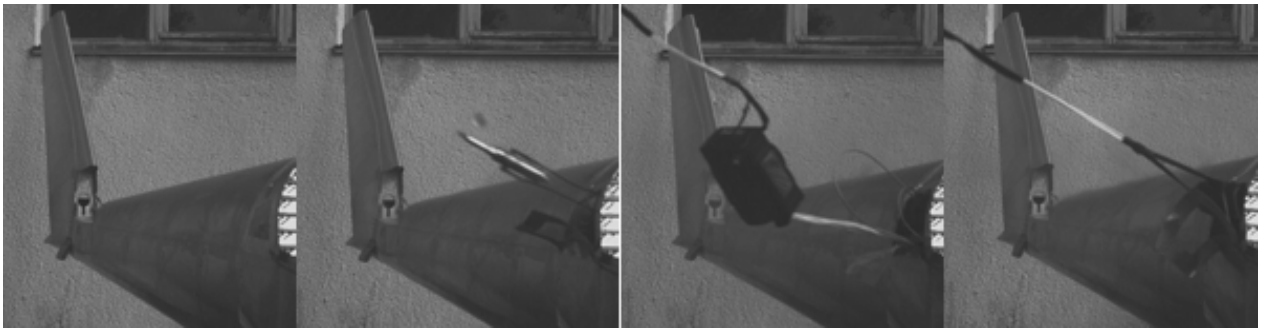

Fig. 1 – Example of IAE testing equipment: Test of Ballistic Recovery System Recorded using High Speed Camera

Apart from education of young engineers, IAE is focused on research and development in aerospace. It has its own significant research capacity and labs. Important part of IAE's research capacity is composed of Ph.D. students. In fact, there is very young research and development team. Research in the Czech Republic took great advantage from joining European Union – in May 2004. Today, IAE is commonly involved in numerous European project, especially in aviation (for example UAVNET, DATON, CESAR, CELPACT, PPLANE, CEDESA, DAEDALOS, etc.). On domestic field, IAE focuses on supporting Czech aviation industry. Typical products of Czech aviation industry are, apart from military training and light combat aircraft, also general aviation aircraft. IAE participated on practical design and testing of wide range of airplanes.

IAE has constantly research and engineering staff of 30+ researchers and engineers, highly skilled in different branches of aerospace design. These include mostly Ph.D. and MSc. degree researchers and engineers, and significant number of professors and associated professors based on Brno University of Technology. IAE

has also close cooperation with many non-aerospace branches on second biggest technical university in Czech Republic.

Despite the fact, that Czech Republic is very short time (since 2008) member of European Space Agency (ESA), IAE has already several space activities. Most important activities are:

A) Space Activities within Aerospace Research Centre

B) Cooperation with ARTI on reliability analyses for space microaccelerometer

C) Participation in EU project SPARTAN

D) Cooperation with Czech partners on ESA call for tenders

A) Space Activities within Aerospace Research Centre

IAE is the coordinator of Czech Aerospace Research Centre. Activities of this centre are described into the detail in chapter 3.

Fig. 2 – IAE initiated and supported development of wide range of modern aircraft. For example development of VUT100 Cobra was initiated at IAE and carried out in cooperation with EVEKTOR company [photos Jan Fridrich and Evektor Co.]

B) Cooperation with VZLU on reliability analyses for space microaccelerometer

IAE closely cooperates with Aerospace Research and Testing Institute in Prague (ARTI) on safety and reliability assessment of microaccelerometer for space use. In particular, it participated on assessment of mechanical part of the device. Whole assessment was done in accordance with ECSS-Q-40B, ECSS-Q-30B and ECSS-Q-30-02A standards. Also, extensive reliability databases available on IAE were used.

C) Participation in EU within project SPARTAN

Project SPARTAN, supported by European Commission within 7.FP is focused on development and demonstration of new propulsion technologies enabling soft and precision landing during planetary missions. IAE participates in the project.

D) Cooperation with Czech partners on ESA call for tenders

IAE actively cooperates with research and industrial partners on preparation of proposals for ESA calls for tenders. As an example, IAE took part in proposal "Universal Modular Reusable Satellite Integration Platform" within AO/1-6052/09/NL/CBI. Proposal was prepared by TC Inter-informatics with participation of Frencken Brno, BUT-IAE and EADS Rostock System-Technik GmbH.

IAE staff supervised also several final projects of MSc. students dedicated to design and stress analyses of mechanical structures for space devices. It also provided background for education of several Ph.D. students focused on space topics.

3 Czech Aerospace Research Centre

Most of aerospace research activities were historically focused on the support of the national aviation industry. Since most of the Czech aerospace products are aircraft in General Aviation category, the research is primarily focused on this area. Major research centres in Czech Republic can be found in Prague and Brno. Fig. 3 shows key research institutes focused on aerospace research in the Czech Republic:

- Institute of Aerospace Engineering, Brno University of Technology (IAE) – coordinator of ARC
- Aeronautical Research and Test Institute, Prague (ARTI) – 1st principal participant
- Czech Technical University, Prague (CTU) - 2nd principal participant

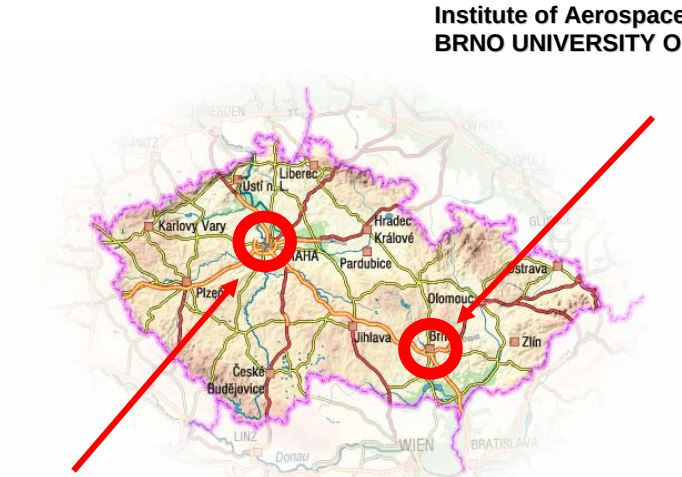

Aeronautical Research and Test Institute, Prague
Czech Technical University, Prague,
Department of Automotive, Railway and Aerospace Engineering

Fig. 3 – Location of key research organizations within Czech Republic

Above mentioned major research organizations are also associated in the **Aerospace Research Ce ntre (ARC)**. National ARC was created in an attempt to unite aerospace research within Czech Republic. It is financially supported by Ministry of Education, Youth and Sports. The project includes all abovementioned key research institutes under the lead of *Brno University of Technology*. Structure of the centre is shown on the figure 4. List of workpackages covers all important areas of aerospace design, manufacturing and operation.

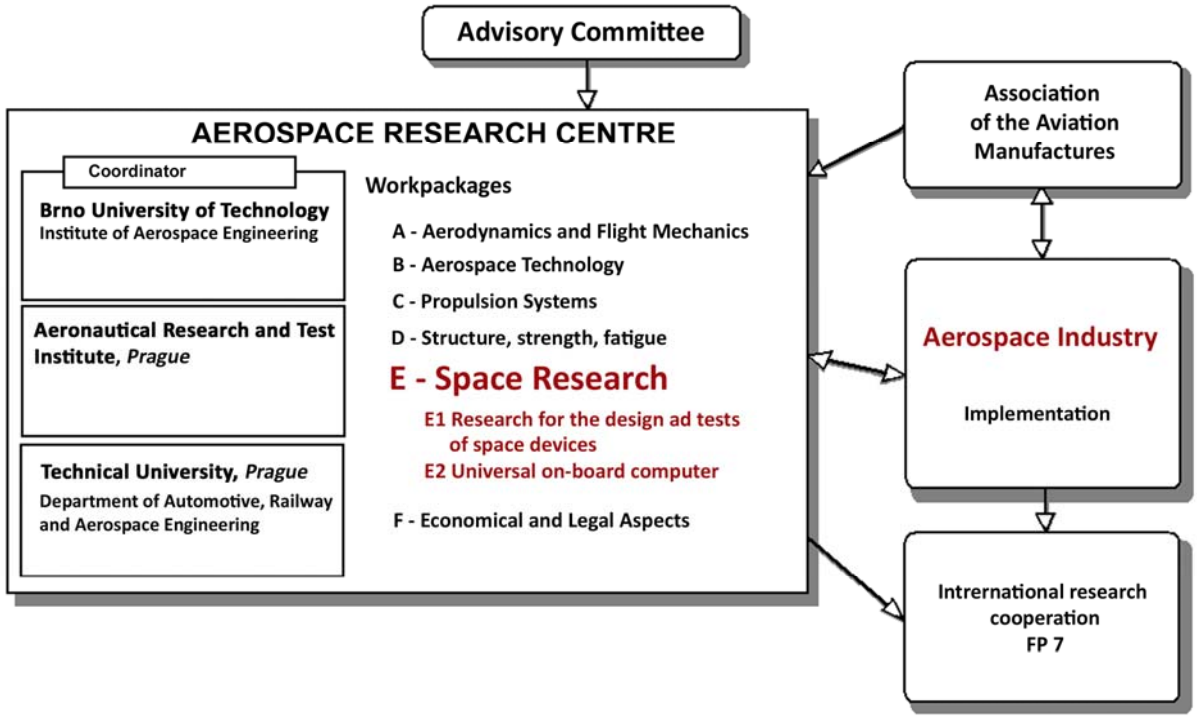

Fig. 4 – Structure of Aerospace Research Centre

ARC is able to support producers during whole design process starting from preliminary analyses and calculations through technological solution for manufacturing plants to testing of prototypes. **Apart from strong areas dedicated to aviation, an important part was also dedicated to space research. Major part of space activities within ARC is carried out by ARTI with significant contribution from IAE. Current space activities in ARC support project of "space microaccelerometer", one of largest and most visible space projects in Czech Republic.** Activities generally include development of methods for design and testing of space devices, safety and reliability analyses and standardization issues. Activities are divided into following groups:

E – Space Research

- E1 – Research for the Design and Tests of Space Devices
- E2 – Universal on-board computer for the use in aerospace and aviation technologies

Particular activities include:

- Calibration of space devices for non-gravitational forces measurements (both on Earth and on orbit)
- Mathematical modeling and computer simulations of space environment influence on space devices
- Reliability analyses of space devices
- ESA and NASA standardization, GOST standardization – analysis, implementation

All abovementioned activities were practically applied on developed micro-accelerometer for space use.

Apart from workpackages directly focused on space devices, several other activities can also be utilized in space research, i.e. activities within Wokpackage B related to development and testing of modern materials, and to environmental issues connected to life-cycle. Also safety and reliability assessment activities can be directly linked to space devices (as was already done for micro-accelerometer).

4 Summary and conclusions for cooperation opportunities

The paper gives an example of space related activities carried out by most important research and academic establishments in Czech Republic. Also space activities in other branches exist in limited manner on Czech academic institutions. For example, research in electrotechnic devices exists at different faculties of Czech Technical University in Prague and also at Brno University of Technology.

Additionally, the paper shows opportunities for cooperation of industry and research partners joined in Czech Aerospace Research Centre. It clearly shows that even before full membership of Czech Republic in ESA, several space oriented research activities existed.

Apart from direct development of space devices and apart from sensors for measurement of physical quantities, great space can be seen in design of ground equipment (jigs, devices for manipulation, testing of partial components for space devices). This can be done using existing infrastructure and using significant experience from aviation applications. Also testing of structures in preliminary development phases using aviation testing labs may be effective and promising (for applications not requiring clean rooms). Such tests can safe significant amount of resources dedicated to early development phases.

Additionally, knowledge in particular areas is available for space projects - for example stress analyses of space structures, or very promising area of safety and reliability assessment. In both areas, IAE has extensive knowledge form aviation applications. Furthermore, in both areas it practically performed work focused on space devices.

Institute of Aerospace Engineering welcomes and appreciates space related cooperation with industrial partners, research establishments and

academia. IAE understands space oriented activities as natural and logical extension of knowledge gained in aviation. Existing experience on IAE ensures mutual benefit for all partners involved in eventual cooperation. Furthermore, partners cooperating with IAE have a bonus in the form of direct access to highly skilled perspective aerospace engineers. Different forms of Bc., MSc. or Ph.D. students involvement in space projects are supported by BUT. Abovementioned opportunities create motivation for potential partners on the space field to cooperate with IAE.

References:

[1] **ECSS-Q-40B** Space Product Assurance – Safety; ECSS (ESA-ESTEC Requirements & Standards Division), Netherlands, ISSN 1028-396X; 17 May 2002

[2] **ECSS-Q- 30B** Space Product Assurance – Dependability; ECSS (ESA-ESTEC Requirements & Standards Division), Netherlands, ISSN 1028-396X; 8 March 2002

[3] **ECSS-Q- 30-02A** Space Product Assurance – Failure Modes, Effects and Criticality Analysis; ECSS (ESA-ESTEC Requirements & Standards Division), Netherlands, 7 September 2001

[4] J.Hlinka: *Failure modes and effects analysis (FMEA) for microaccelerometer MAC-04 locking mechanism*, LÚ 52/2006, 24.02.2006

[5] J.Hlinka: *Failure modes and effects analysis (FMEA) for microaccelerometer MAC-04 mechanical structure*, LÚ 51/2006, 24.02.2006

[6] **Czech Space Office** [online]; 2010 [cit. 2010-08-13] Available at: www.czechspace.cz

HTHL Space Launch Vehicles: Concepts, Advantages and Control Problems

Prof. Dr. Alexander Nebylov, International Institute for Advanced Aerospace Technologies of State University of Aerospace Instrumentation, Saint-Petersburg, Russia

Integrated launch systems that include aerospace plane (ASP) and another great winged vehicle (plane or better ekranoplane) as a booster are reviewed. It is shown that ekranoplane with mass of 1500 ton or more is capable to carry ASP with initial mass of 500 ton and landing mass of 60-70 ton. Ekranoplane can provide ASP with the primary speed of Mach 0.5-0.65 in required direction that allows to lower the requirements to ASP wing area and its engines. A number of other advantages of the offered transport system are connected with possible using the ekranoplane at ASP landing. Heavy ekranoplane is the unique vehicle for realization the progressive idea of docking to descending ASP the stage allowing to expand opportunities of its landing. The problem of ASP horizontal landing without undercarriage by docking with other flying vehicle at the last stage of decent and the requirements to control systems are discussed.

1 Introduction[1]

The cost reduction of useful mass injection into near-Earth orbit, expansion of functionality of space transport systems and ecology safety requirements are among the major problems of space engineering. The fully reusable single-stage-to-orbit (SSTO) aerospace plane (ASP) with horizontal launch and landing might be ideally applied to meet such requirements. However, other demands and limitations, which bound with the state of the art of necessary technologies and forecasting of future technological level, force to consider a SSTO ASP only as a purpose which can be achieved stepwise. On the near-term steps of ASP improving it is necessary to consider them as a part of integrated space transport system.

Among two methods of ASP launching into orbit, vertical take-off (VT) and horizontal take-off (HT), presently VT takes the lead from HT. The decisions for the X-33 program by NASA, for HOTOL by British Aerospace, for MAKS by RSA also, seems to favor VT (but modern designs of Skylon, and SpaceShipOne again give chances to HT). In retrospect, almost all of the launch vehicles in the past have been VT. However, broadening the range of requirements for space transportation systems seems to favor the need for HT.

[1] The work was supported by the Russian foundation for Basic Research under the project 09-08-00529-a.

The project of ekranoplane (or Wing-in-Ground effect vehicle or WIG-craft) use for horizontal launch and landing of ASP was offered by N. Tomita, Y. Ohkami and A. Nebylov in 1995 [1,2] and since that time it has been developed in a view of detailed reasoning and feasibility study [3-9]. The goal of investigation is the creation of space transportation system with reduced specific cost of payload injection at LEO or MEO and extended functional capacity.

2 Concept of ASP-Ekranoplane launch system

What are the reasons to use the ekranoplane as an additional component in space transportation system that assists at ASP landing? Three main reasons may be pointed.

1) The landing point can be chosen at any area of ocean that gives wide possibilities for ASP landing trajectory selection.
2) ASP can be supplied with simplified and lighted landing gear or has not gear at all when landing on ekranoplane, moving with the velocity equal to ASP one. Extremely large saving of mass will be provided if all equipment for docking is an accessory of ekranoplane. The mass of gear for landing on runway may be approximately 3% of empty mass or 25–30% of payload. So, ekranoplane use can increase the payload of ASP on 30% and to decrease accordingly the specific cost of launch.
3) The cosmodrome with specially prepared runway is not required.

The problem of ekranoplane's type choice for ASP-Ekranoplane system is very relevant. The generally accepted classification of ekranoplanes involves three types. The ekranoplanes of a type A can move only in the zone of WIG-effect strong action at the altitude approximately equal to a half of the wing chord or less. Ekranoplanes of a type B have an elevator and flaps that allow to select an optimal altitude from a coverage of WIG-effect, and also to accomplish the transient increasing of the flight altitude in the mode «dynamic zoom». The ekranoplanes of a type C can fly not only at the altitudes of WIG-effect action, but also in an airplane mode. For this purpose they should mate aerodynamic and design qualities of ekranoplane and airplane, that as a matter of fact results in impairment of both capacities.

If it is necessary to cause an airplane to use sea surface as an aerodrome, for this purpose there is a well-known and very successful engineering solution called a seaplane. But a heavy ekranoplane with a wing of small length factor and special profile, with "under-blowing" engines, with a ship-type body of corrosion-resistant metal, with different means of longitudinal stability maintenance in a WIG mode of flight and good stiffness afloat, must not compete against airplane in the ocean of air, it would be not logically. Of course, it is possible to construct an ekranoplane of a type C, but at a large take-off mass such an ekranoplane will be too expensive and having restricted effectiveness. At the same time the heavy ekranoplanes of a type B with good seaworthiness are promising in several applications [8].

Therefore the ekranoplane of a type B has to be used in the project "ASP-Ekranoplane".

Nine variants of ASP landing with ekranoplane assist were analyzed [4]. The variant of ASP landing to the deck of moving ekranoplane by the use of docking and mechanical mating is the most interesting and produces the most harsh demands to motion control systems accuracy and reliability.

3 Requirements to ekranoplane

The demanded carrying capacity in 530-700 ton with a mass ratio about 35% determines ekranoplane take-off mass in 1600-2000 ton. By accepting specific loading on a wing of 5-6 kN/m^2, one can estimate the required area of ekranoplane wing *S* in (3-4)10^3 m^2. With conditional lengthening of the wing λ=3-4 the wing length should make $L = \sqrt{S\lambda}$ = 90-110 m.

With the normal thrust-to-weight ratio of ekranoplane in 25% the total trust of engines should be of the order (4-5)10^3 kN, which can be ensured by 6 engines with a single thrust of 600-800 kN. As it is important to raise the speed of starting ASP to maximum, it is expedient to involve in this mode all engines, as well as at ekranoplane take off. The criterion of fuel saving is not paramount for ekranoplane-launcher. However, the stock of fuel should ensure an opportunity of ferry flight for a distance no less than 3000 km.

Seaworthiness of the ekranoplane with linear dimensions about 100 m and mass of 2000 ton can be defined from the experience of Russian ekranoplanes "Lun" and "KM" operation, which with the mass approximately 400 ton have confirmed sea-worthiness in 5 numbers appropriate to allowable height of a wave with three-per-centage providing in 3.5 m. The factor of recalculation can be determined under the Frude's formula as a cubic root of the relation of weights, that is (2000 / 400) 1/3 = 1.71. It gives allowable height of wave 3.5m *1.71 = 6.0 m that corresponds to seaworthiness in number 6 for the modes of take off and landing.

Similarly one can estimate achievable maximal speed of large ekranoplane-launcher in 600-650 km / hour, though basically the value of 550 km / hour can appear quite sufficient, and the optimal landing speed lies inside the interval 400-550 km / hour. At last, ekranoplane as the control plant should have a good margin of stability and react poorly to any variations of loading and other disturbing forces and moments arising basically at ASP start. The stiffness and correct centering of floating ekranoplane should be also supplied.

It is clear, that the given requirements cannot be executed in the framework of the well-explored plane configuration of ekranoplane "a carrying wing + tail assembly" even with essential increase of the dimensions in comparison with ekranoplane "Lun". It is also clear, that ekranoplane-launcher should be catamaran. The possible design of "combined wing type" ekranoplane with ASP is shown in Fig. 1.

For ASP launch ekranoplane (1) carries it to the chosen point of start which may be several thousand kilometers apart, (2) refuels ASP with the components of liquid propellant directly before start having onboard powerful cryogenic equipment and tanks for liquidized gas and (3) gives to ASP the initial velocity M=0.5-0.65 at the altitude of 10-20 m. In this case ASP in compare with MAKS project obtains less mechanical energy, but in recalculation to the attainable final velocity this loss does not exceed a few percents [2-4]. A buster main goal is connected with jumping over the zone of small velocities which is unacceptable for hypersonic wing and engines, and ekranoplane masters this role well.

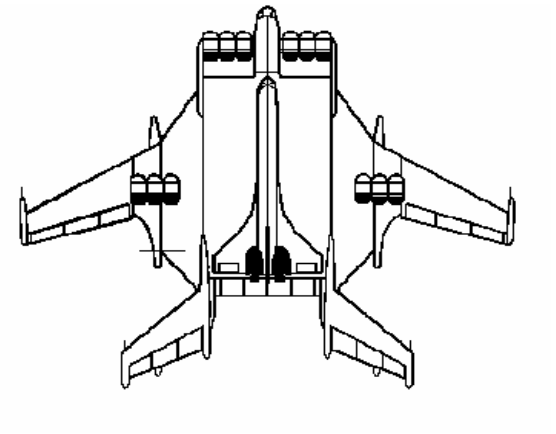

Fig. 1 - Ekranoplane of "Combined Wing" configuration with docked ASP

4 Arrangement of mechanical docking elements

The initial position of fueled ASP on the ekranoplane deck has to be practically horizontal and close to the deck to reduce the aerodynamical drag during ekranoplane take-off and cruising flight to the area of ASP launch. At the moment of ASP engine switching on the ASP must receive around 15º attack angle [3-4] and some space between the engine muzzle and the ekranoplane deck. That means that ASP center of gravity is elevated for approximately 10m and, probably, the whole ASP is shifted a bit back to locate the engine muzzle in the free space.

Such initial elevation of ASP could be provided by rather powerful mechanism, which applies lifting force at the area of ASP center of gravity. It may be the extensible hydraulic column that could produce the force in 5000 kN and to be rather stable against longitudinal aerodynamical force applied to ASP connected with ekranoplane motion. Practically this column has to carry the ASP weight minus aerodynamic lifting force of ASP wing. Another important requirement to the undocking mechanism consists in minimal disturbed forces and moments applied to ASP at its disconnection with ekranoplane. The ASP weight must be balanced by its wing lifting force. Any turning moments in the longitudinal plane must be canceled out by the right deflection angles of the elevator and flaps. That is reason for the ASP attitude stabilization system to be switched on before the launch. ASP engine thrust has to approximately balance a drag force. So, ASP engine has to be switched on also before ASP disconnection with ekranoplane.

Taking into account the listing of above requirements, the arrangement of mechanical mating elements for connection and disconnection of ASP with ekranoplane can be drawn out as it shown in Fig. 2.

The central extensible column CC is the main facility at ASP launching procedure. It is buried deeply into ekranoplane body during ASP transportation to the launch

area, but arises at maximal height of around 10m before ASP undocking. It is not necessary for CC column to manage the ASP pitch. Directly before undocking this function will belong to ASP flight control system. But for preset ASP the initial angular position and for partly help CC column in load carrying two or three another connecting elements will be used. For example, it could be a nose column NC and two tail columns TC1 and TC2. NC is located on the central line in a forward part of the Ekranoplane deck.

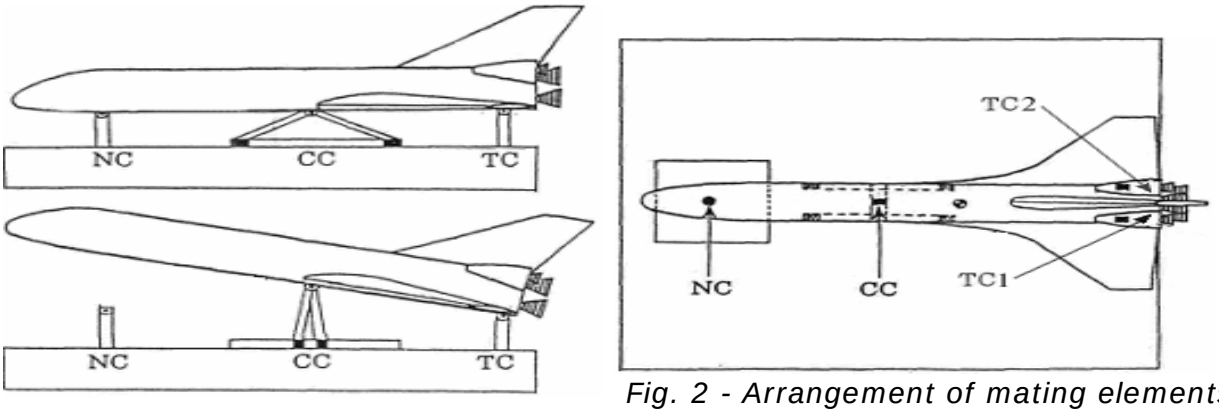

Fig. 2 - Arrangement of mating elements

5 Motion control at docking

A generalized scheme of automatic control multi-dimension digital system for mutual motion control at docking is shown in Fig. 3. As it follows from the diagram, the docking process of ASP and ekranoplane must be operated under motion control complex which involves closed control loops for ASP and ekranoplane absolute motion with controlled values matrices λ_{ASP} and λ_{EKR} consequently, relative motion closed control loop with the controlled value matrices λ_{ASP} - λ_{EKR} and an additional open loop channel for local shifting the docking element along and thwart landing deck with output coordinates matrix λ_M. The required landing trajectory of ASP is determined by synthesizer priory and described by given functional matrix $\lambda(t)$. The navigation system of ASP generates an estimation of an actual motion trajectory $\lambda_{ASP}(t)$. The residual $\lambda(t)-\lambda_{ASP}(t)$ is used in control law. Optimization allows to reduce a norm of the matrix $\lambda(t)-\lambda_{ASP}(t)$ and to provide the high accuracy in holding the required landing trajectory. At the final stage of approach the errors of relative positioning may be within 2-3m, and the local positioning of matting elements (especially, nose element) could reduce the errors to 30cm.

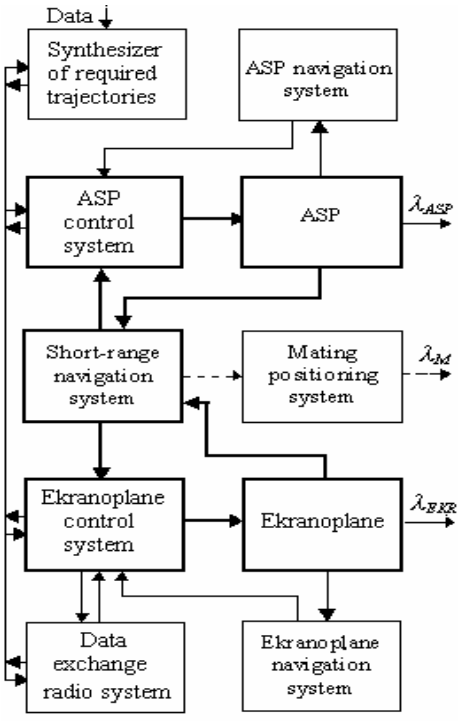

Fig. 3 – Motion control complex

The ekranoplane absolute motion control system has to ensure the required trajectory of its flight to the point of ASP landing, approach to this point from given direction at required time, and the capture of ASP by the short-range optical navigation system.

6 Conclusion

- ASP with ekranoplane assist at horizontal take-off could be competitive with vertical space launch system from aggregate functional, technological and life cycle cost viewpoint.
- Ekranoplane with perfect control system can realize the idea of docking the stage that would allow ASP landing without gear.
- The accurate and reliable control of relative motion at undocking and docking is the key problem of ASP-Ekranoplane integrated space system feasibility.

References:

[1] Tomita, N., Y. Ohkami: *A study on the application of take-off assist for a SSTO with rocket propulsion*; IAF-95-V.3.06. 1995

[2] Tomita, N., Nebylov, A.V. et al.: *Feasibility study of a rocket-powered HTTL-SSTO with ekranoplane as takeoff assist*; 7th AIAA International Aerospace Planes and Hypersonic Technologies and Systems Conference. Norfolk, USA, AIAA 96-4517, 1996

[3] Tomita, N., Nebylov, A.V. et al.: *Performance and Technological Feasibility of Rocket Powered HTHL-SSTO with Take-off Assist*; Acta Astronautica, 45, No. 10, pp. 629-637. 1999

[4] Tomita, N., A.V. Nebylov, V.V. Sokolov, Y. Ohkami: *Performance and technological feasibility study of rocked-powered HTTL-SSTO with takeoff assist*; 47th International Astronautical Congress, Beijing, IAF 96-V.3.05. 1996

[5] Nebylov, A.V.: *WIG-Flight Automatic Control Principles, Systems and Application Advantages*; 15th IFAC Symposium on Automatic Control in Aerospace. Forli, Italy, pp. 542-547. 2001

[6] Nebylov, A.V.: *Controlled flight close to rough sea: Strategies and means*; In: 15th IFAC World Congress, Barcelona, Vol. 8a. 2002

[7] Nebylov, A.V., Nebylov, V.A.: *WIG-Craft Marine Landing Control at Rough Sea*; Proceedings of the 17th IFAC World Congress. Seoul, Korea, pp.1070-1075. 2008

[8] Nebylov, A.V. and Wilson P.: *Ekranoplane - Controlled Flight close to Surface*; Monograph; WIT-Press, UK, 320 pp.+CD. 2002

[9] Nebylov, A.V.: *Principles and systems of heavy WIG-craft flight control*; Proceedings of 18th IFAC Symposium on Automatic Control in Aerospace; Nara, Japan, 2010

Active Noise Control in Military, Civil and Space Applications

Ing. Jaroslav Hovorka, Mesit přístroje spol. s r.o., Uherské Hradiště

Acoustic Noise problems are troublesome for the crewmembers of a broad range of military, civil and space platforms. These platforms can be combat vehicles, trucks, airplanes and space ships. Disturbing noises are generated by a wide range of equipment, however mainly they are coming from engines, fans, compressors, transformers, moving parts, etc. Crewmembers working inside these platforms or people working in close proximity to these platforms are exposed to extremely high acoustic noise levels for a very long time. These noises enter communication systems and interfere with the speech. As the result of this, the noises significantly degrade speech intelligibility and can damage hearing and destroy the health of individual crewmembers. It is absolutely necessary to attenuate these noises to the acceptable level. This level is given by the international standards. If efficient noise attenuation is reached, crewmembers do not suffer from hearing damage when working inside such a noisy area. The traditional approach to acoustic noise reduction uses only passive techniques. These passive techniques are widely used, however physical limits exist. They can reach reasonably good noise attenuation over a broad frequency range, however they are completely ineffective at the low frequencies. Passive techniques are also large and very expensive. Acoustic noise levels at the low frequencies are extremely high in reality. It is generally known, low-frequency noise is very annoying for the crews and it can cause fatigue and loss of concentration. This can have very serious consequences and cause critical situations resulting in serious accidents. It is clear, sufficient noise attenuation cannot be reached only with passive technology in reality. In an effort to overcome the problems with traditional passive approach, Active Noise Control (ANC) is implemented. In Active Noise Control, secondary sources are used to cancel noise coming from the primary noise source. Active Noise Control incorporates an electro-acoustic system cancelling unwanted noise on the principle of superposition. Active Noise Control is achieved by generating a cancelling signal through secondary sources. These sources are connected to Digital Signal Processing system where specific noise cancelling algorithm is implemented on digital signal processor. This way it is possible to reach reasonable noise attenuation compared to passive technology. Active Noise Control is developing very rapidly today. It provides advantages such as size and weight reduction, which is very important mainly in military and space applications. In this paper, basic understanding of the noise levels, noise reduction and noise control methods and algorithms suitable for the military and space applications is given.

Noise inside the very noisy platforms

There are a broad range of noise generators on the board of vehicles, airplanes and spaceships.The most important noise sources are engines and all the assemblies of moving parts. In case of a combat platforms, significant noise is also generated by the operation of weapon stations. Definitely, significant noise is also generated by the movement of the platform.

Noise levels

Noise inside the platform can reach extremely high sound pressure levels (SPL). For example, noise level inside the tracked vehicle moving at a speed of 40 km/h can reach up to 117 dB at 63 and 125 Hz octave bands [1]. These noise levels can cause hearing damage to the crew if exposed to such a noisy environment during the work shift. This is the main reason, effective ways are being searched today to suppress such levels and prevent hearing damage to the crew.

f [Hz]	63	125	250	500	1000	2000	4000	8000
SPL [dB]	117	110	104	96	92	88	80	75

Table 1 - SPL measured inside the tracked vehicle [1]

Noise exposition prediction

It is very difficult to make real noise measurement on the board of a particular platform (vehicle, airplane, …). The goal is to measure noise exposition of a crew when wearing personal protective headset or noise protector. By the way, one of the reasons is that very expensive measuring apparatus can be destroyed during measurement, for example when measuring is made inside the combat vehicle moving in a heavy terrain. One possible way to find the Noise Exposure of a crew is to use prediction [1].

Here is a basic equation for the calculation of Noise Exposition [1]:

$$L_3 = 10.\log\left(\frac{1}{T}.\sum_{i=1}^{n}\left(t_i.10^{\frac{L_i}{10}}\right)\right) \quad [dB(A)] \qquad (1)$$

Where L_3 is Noise Exposition for a period of time T, T is a total time crew is exposed to the noise, Li is SPL affecting the crew for the period of t_i.

Excessive noise attenuation

There are two basic ways to make the life of the crew easier and to protect their health. All the crew is equipped with personal headset providing not only communi-cation to onboard communication systems, however the most important feature of

the personal headset is its capability to significantly attenuate noise levels. However, physical limits exist when designing a personal heaset. It is practically impossible to reach sufficient attenuation of low frequency noises. Results [1] of real measurements state that the noise levels up to 500 Hz are significant. So the passive attenuation of personal headset is not enough to guarantee good working conditions for the crew.

The only possible way to increase total attenuation of the noise protector or a personal headset is to use electronic circuitry which adds additional noise attenuation mainly at the low frequencies. This can be done with analog circuits - Active Noise Reduction circuitry (ANR), or with digital signal processing algorithms – Active Noise Control (ANC) [2],[3].

Active Noise Reduction

Active Noise Reduction, see Figure 1 is an electronic feedback circuit which gives additional attenuation to the personal hearing protective device. Noise sensing microphone is placed inside the headset close to the input of the ear canal. This microphone picks up residual noise penetrating through eashell of the personal headset. This signal picked up by Noise Sensing Microphone is filtered by low-pass filter, amplified and fed back to the sum amplifier where is subtracted from the input speech coming from headset close-talking microphone. Resulting signal is amplified and fed to a headset speaker. The principle of this method is to generate antinoise wave which cancels the noise penetrating to the ear canal through the eashell of a personal headset.

This Active Noise Reduction is implemented in personal headset manufactured by Mesit přístroje spol. s r.o. This feedback circuitry is implemented in one electronic module, which is inserted inside the personal headset, see Figure 2. It is possible to add approximately 15 dB of additional attenuation to passive attenuation of the headset. ANR circuitry is working up to 500 Hz, which is the drequency band of interest.

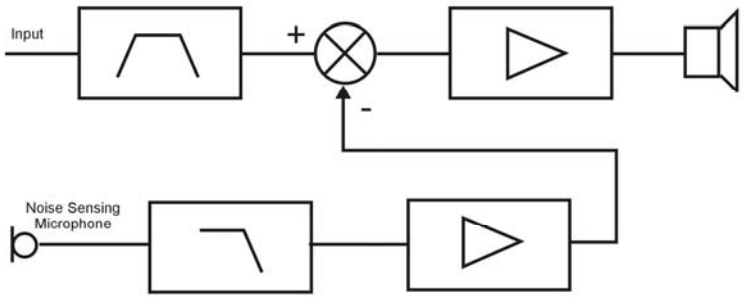

Figure 1 - Active Noise Reduction Loop

Figure 2 - Active Noise Reduction module inside personal headset

Active Noise Control

The second possible way to add additional noise attenuation is to implement Active Noise Control (ANC). This can be implemented with a broad range of digital signal processing algorithms and Adaptive Filtering is used. Basic schematic for ANC can be seen in Figure 3 [2].

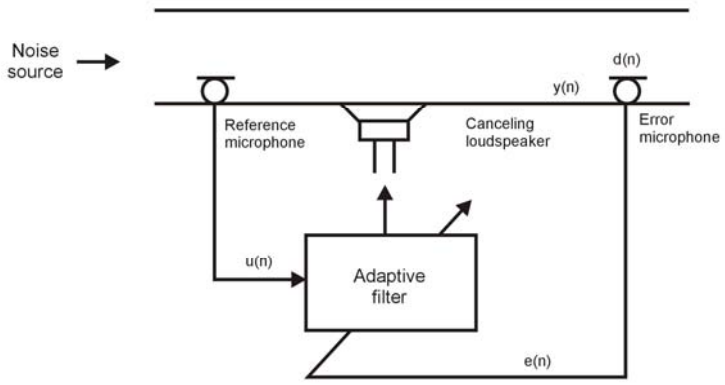

Figure 3 - Active Noise Control

There is a reference microphone placed close to the source of the noise. The task of this reference microphone is to pick up this primary noise $u(n)$ coming from the noise source. However, primary noise is also going to the error microphone.

The role of the canceling loudspeaker is to generate the so called canceling wave, antinoise signal. This wave also propagates to the error microphone. This canceling wave must be of the same amplitude as the noise signal, but the opposite phase to cancel the primary noise. The residual noise picked up by the error microphone is used to update the coefficients of the Adaptive Filter. In reality, in the headset, ANC

application is really very difficult, placement of the reference and error microphones plays a key role together with the shape and volume of headset earshell.

Subband Adaptive Filtering

The main drawback of using classical adaptive algorithms in ANC is very high computational load and as a reason of this, slow convergence of the algorithm. As the reason of this Suband Adaptive Filters (SAF) are widely used in these algorithms. Basic block diagram of SAF can be seen in Figure 4 [2].

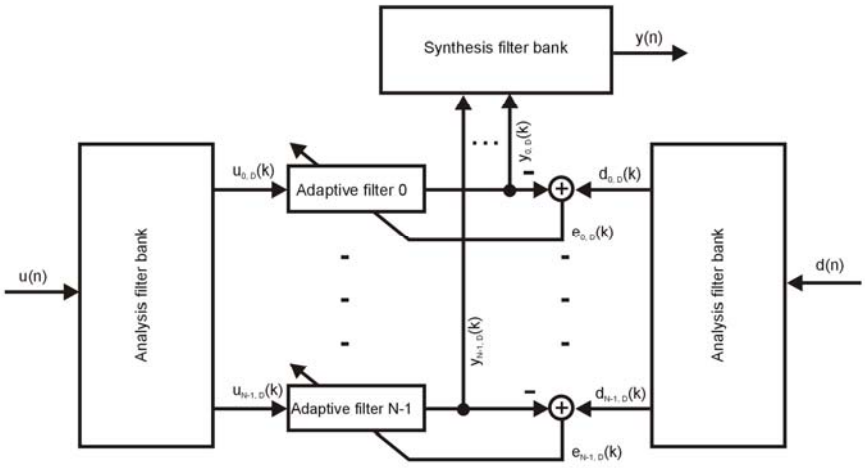

Figure 4 - Subband Adaptive Filtering [2]

In [2] an analysis of computational reduction of SAF compared to fullband filtering is done.

Computational savings can be expressed [2]:

$$\frac{Complexity\ of\ \ fullband\ \ filter}{Complexity\ of\ subfilters} = \frac{D^2}{N} \qquad (2)$$

Where D is decimation factor, N is total number of subbands. If $D = N$, greatest computational savings are reached (critically sampled SAF).

SAF partitions both the fullband input $u(n)$ and desired $d(n)$ signals into N subbands. These subband signals are decimated from the original sampling rate f_s to the lower sampling rate of f_s / N.

Advantage of this solution in comparison to ordinary fullband adaptive filter is that the long M -tap filter is replaced by N FIR filters with less taps. These filters are operated in parallel. Fullband $y(n)$ signal is the output of Synthesis filter bank. Synthesis filter bank is composed of a bank of interpolators. These interpolators

must upsample the subband signals $y_{i,D}(k),\ i=0,1,...,N-1$, before filtering and adds these signals together.

One of the drawbacks of the SAF is introduction of substantial delay in a signal path. The cause of this delay are Analysis and Synthesis filter banks.

SAF basic structures

There are two main SAF structures [2] depending on the derivation of the error signal.

- Open-loop structure
- Closed-loop structure

Open-loop structure

The input signal $u(n)$ and desired response $d(n)$ are particioned into subbands by identical analysis filter bank, $H_i(z), i=0,1,...,N-1$. Then these signals are decimated by factor D. In each subband decimated signal $u_{i,D}, i=0,1,..N-1$ is filtered by an adaptive subfilter $W_i(z), i=0,1,...,N-1$. Output of this subfilter is compared with the corresponding desired response. Resulting subband error signals $e_{i,D}, i=0,1,..N-1$ are used to update the associated adaptive subfilters.

In the open-loop structure, see Fig. 5, coefficients of the individual subfilters are adapted in its own adaptation loop. This way it is minimized local MSE in each subband. These local subfilters operate absolutely independently.

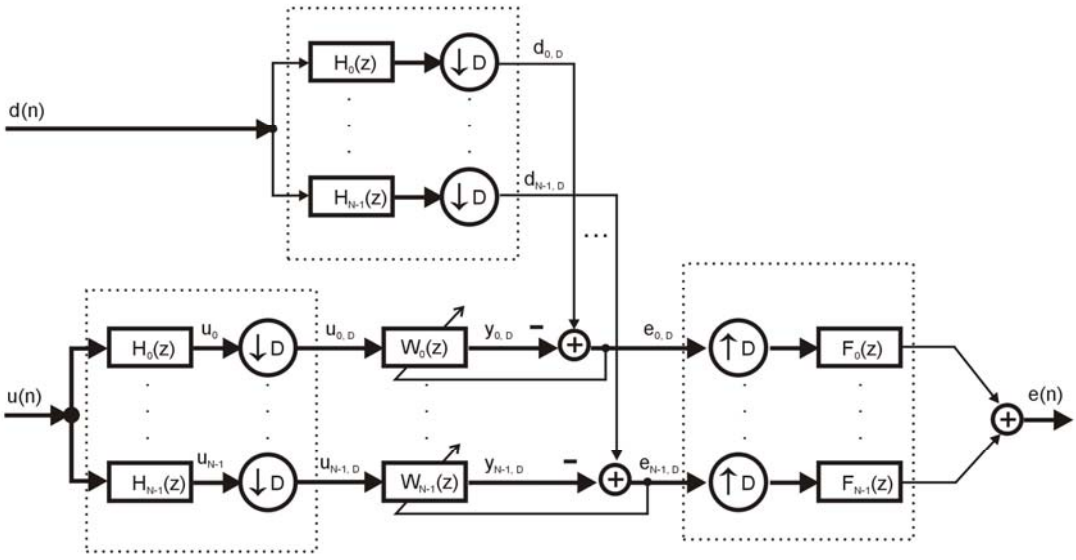

Figure 5 SAF – Open-loop structure

Closed-loop structure

Closed-loop structure [2] can be seen in Fig. 6. Input signal $u(n)$ is partitioned into subbands – filters $H_i(z), i=0,1,...,N-1$. Filtering of the input signal $u(n)$ is done in these subbands. Fullband output signal $y(n)$ which is the sum of the outputs of synthesis filters $F_i(z), i=0,1,...,N-1$ is compared to the delayed desired response $d(n)$. Result of this comparison is error signal $e(n)$, which is partitioned into subbands using the analysis filter bank $H_i(z), i=0,1,...,N-1$. These subband error signals are decimated and then these error signals $e_{i,D}, i=0,1,..N-1$ are used for the adaptation of the respective adaptive subfilters.

Significant advantage of a closed-loop structure is that it minimizes the fullband MSE instead of independent MSE of individual subfilters.

Closed-loop structure minimizes the fullband error signal and guarantees that adaptive subfilters converge to the optimal Wiener solution.

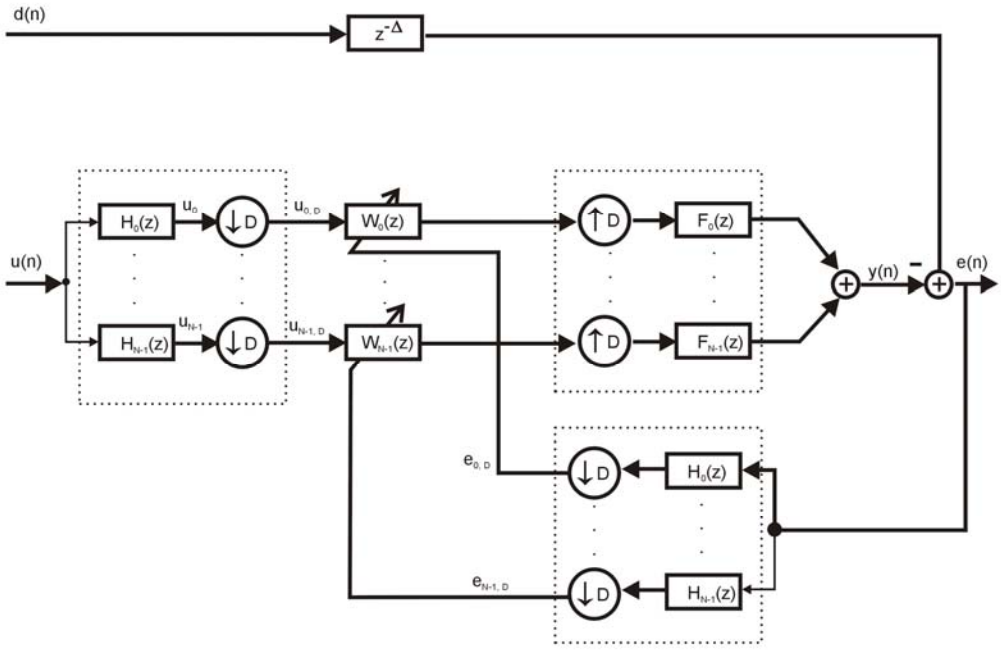

Figure 6 SAF – Closed-loop structure

Conclusion

Noise inside a broad range of moving platforms is a significant problem for the crew. Crew members use personal headsets which attenuate extremely high nois elevels. Only passive attenuation is not enough and this is the reason Active Noise Reduction and Active Noise Control are implemented. Active Noise Control is digital algoritm

which uses Adaptive Filtering. However, only pure adaptive filter suffers from high complexity and slow convergence. Subband Adaptive Filtering is used to reach better convergence in reality. Wide range of SAF algorithms exist, either open-loop or closed-loop. Great advantage of closed-loop structure is that it minimizes the fullband MSE as opposed to the open-loop structure. New structures are being investigated.

References:

[1] Hovorka J., Marko M., *Predikcia hlukovej expozície osádky bojových vozidiel*; Zborník prednášok zo XVII. Odborného seminára BEZPEČNOSŤ PRÁCE na elektrických inštaláciách a elektrických zariadeniach, SES Liptovský Mikuláš, 2009

[2] Lee Kong-Aik, Gan Woon-Seng, Kuo Sen M., *Subband Adaptive Filtering Theory and Implementation*; John Wiley & Sons, 2009

[3] Kuo Sen M., Morgan Dennis R., *Active Noise Control Algorithms and DSP Implementations*; John Wiley & Sons, 1996

Software Package Development for Simulation of Complex Flexible Space Vehicles

Dr. Alexander Nebylov, Dr. Alexander Panferov, Dr. Sergey Brodsky,
International Institute for Advanced Aerospace Technologies of State University of Aerospace Instrumentation, Saint-Petersburg, Russia

The concept of developed universal program for research of dynamic properties, calculation of mathematical models, comprehensive simulation of flight and synthesis of control laws for different types of flexible aerospace constructions (launchers and satellites) is considered. The basis of the program is the structure, which allows carrying out of the analysis of dynamic characteristics, simulation, and visual information representation. The software package is supplied with the library of program modules. These modules are designed on the basis of mathematical models of separate vehicle elements and different physical effects, such as flexibility, sloshing, sluggishness of engines, local angle of attack values, etc.

1 Introduction[1]

Possible approaches to the mathematical description of different types of flexible vehicles are observed. Mass and aerodynamic characteristics are changing considerably during the flight of aerospace vehicles. From the point of view of control theory such vehicles are the typical non-linear and non-steady plants [1-4]. The aim of designer is to create the light construction. For these reason such objects are deformed in flight, and their elastic properties appear. Elastic longitudinal and lateral oscillations of the complex form arise, which frequencies are changing during the flight. Elastic oscillations are usually described by differential partial equations or ordinary differential equations of the great dimension. Deformation of a body results in appearance of the local attack angles and slide angles. As a result of it, the local forces and moments of forces arise. These forces and moments are synchronized with the changes of local angles of attack and slide. The local forces and moments are the reasons of amplification or attenuation of elastic oscillations. This phenomena is known as aeroflexibility. At excessive development of elastic oscillations the structural failure may take place. Paying attention to these effects has a great importance at control of space stations and space probes, airplanes and other mobile objects liable to the considerable dynamic loads.

[1] The work has been supported by the Russian foundation for Basic Research under the project No. 10-08-01049-a

Besides the flexibility and aeroflexibility, it is necessary to take into account in the mathematical models of aerospace vehicles the following factors:

1) Dependence of all parameters on time, velocity and altitude of flight, drift of CG, and so on.
2) Distributed and integral aerodynamic forces.
3) Oscillation of liquid in tanks (Sloshing).
4) Inertia of engines.
5) Errors of measuring instruments.
6) Environment stochastic forces and moment of forces.

Mathematical descriptions of all these factors are complex and are based on different physical models [5, 6]. For research of elastic systems the special programs exist, for example, ANSYS, NASTRAN, Coventor, Femlab, Structural Dynamics Toolbox for use with MATLAB, etc.

In these programs the finite element method is used, which has been well recommended at calculation concerning the simple designs. For dynamic processes investigation and also for simulation of elastic oscillations of the flying vehicles, which consist of hundreds and thousand units of complex form, such approach is unsuitable. For calculation of distributed and integral aerodynamic forces can be used the program Fluent. The program Matlab allows to design of control or stabilization system. It is required to use all models simultaneous for analysis of interconnections and detection of possible resonances.

For with reason, the resulting mathematical model is very complex. There are no known programs to analyze and simulate such complex systems which include subsystems, which base on different physical principles.

The indicated reasons determine the necessity of development of the specialized program for simulating the motion of flexible objects of the composite form, the analysis of their dynamic properties and design of control systems.

In the presented paper other approach to modeling and control system design for flexible objects is observed. It is known that the flexible object is described by partial differential equations. The control theory of such objects is complex, bulky and presently is insufficiently designed analytically. There are numerical methods of calculation of the arbitrary quantity of harmonics of flexible vibrations and replacements of partial differential equations by ordinary differential equations of high dimension. For automation of analytical derivation of such mathematical models of flexible aerospace vehicle, for control law synthesis, for analysis and simulation of controlled flight, and also for representation of outcomes of modeling in the two-dimensional and three-dimensional space, the authors have developed the specialized software package.

2 Methods of the problem solution

Authors propose new approach and special program to input construction of aerospace vehicles, to calculate mathematical model, to correct this model on the basis of separate experiments, to simplify separated models for any factors. The program allows using whatever experimental data about properties of the vehicle, presented in the most various formats. Hand-operated input and correction of separate values, and also the automated lead of large arrays of the information is provided. At absence or inaccessibility of a part of experimental data in the program, the models based on various theories or on generalization of experimental data of vehicles are used. The software for simulation of flexible essentially non-steady vehicle motion, synthesis of control systems for such a vehicle, research of dynamic properties by different methods in time and frequency domains, is developed and described in this paper. The basis of the program is the structure which allows analyzing the dynamic responses, simulation and visual information representation of the complex dynamic systems.

All stages of aerospace vehicles design are discussed, including the following problems:

- input of initial constructive data of a vehicle,
- determination of controllability and observability for the full and simplified model of a vehicle for real control inputs and arbitrary choice of measured signals,
- choice of flight program and control law,
- automatic linearization relative to an arbitrary trajectory,
- automate processes of mathematical models simplification for flexible vehicles and separate physical phenomena (oscillations of a liquid in cavities, time lag of engines, local aerodynamic loadings, etc.) and to control these simplifications,
- execute a control system synthesis for elastic object in frequency area with the given margin of stability on amplitude and a phase,
- control system synthesis for a vehicle with use of method of Kalman filtration and methods of optimal control,
- simulation of vehicle motion with nonlinear model and control law different complexity,
- investigation effect of local aerodynamic loadings on elastic vibrations of a vehicle,
- determination eigenfrequencies of a liquid oscillations in tanks and computation of the local forces which are affect on a vehicle body because of these oscillations,
- choice of sensors and actuators characteristics,

- computation charts of relations for any variables of state vector, both from a time and from other variables of state vector,
- any frequency characteristics plots construction,
- choice of flight program and control law,
- determination of the elastic vibrations of a body and oscillation of liquid in tanks modes and to illustrate these oscillations as animations,
- study of control system sensitivity to vehicle parameters change.

3 Mathematical models of physical phenomena having place at flight

3.1 Solid Dynamics

The rigid part of mathematical model of vehicle is allocated into the separate block, in which the system of differential non-linear equations of vehicle spatial motion is integrated. These equations in vector form in body-axes can be written as

$$\frac{d\mathbf{V}}{dt} = \frac{\mathbf{F}}{m} - \Omega \times \mathbf{V}, \quad (1)$$

$$\frac{d\Omega}{dt} = \mathbf{I}^{-1}\left(\mathbf{M} - \Omega \times \left(\mathbf{I} \cdot \Omega\right)\right). \quad (2)$$

These equations express the motion of a rigid body relative to an inertial reference frame. Here $\mathbf{V}$ is velocity vector at the center of gravity (CG), Ω is angular velocity vector about the c.g., $\mathbf{F}$ is total external force vector, $\mathbf{M}$ is total external moment vector, $\mathbf{I}$ is inertia tensor of the rigid body.

Outputs of this subsystem are parameters of vehicle motion as a rigid body.

3.2 Flexibility

Equation of elastic line flexible displacements from the longitudinal neutral axis looks like

$$\Delta \mathbf{M}\ddot{\mathbf{q}} + \Delta \Xi \dot{\mathbf{q}} + \mathbf{q} = \Delta \mathbf{f}, \quad (3)$$

where $\mathbf{q}(t)$ is deflection of elastic line from the longitudinal axis; Δ is symmetrical stiffness matrix; $\mathbf{M}$ is diagonal mass matrix; Ξ is symmetrical structural damping matrix; $\mathbf{f}$ is distributed load.

3.3 Aerodynamics and local loads

The distributed and concentrated forces appear because of formation and a break-down of a vortex on the vehicle surface.

Local aerodynamic effects substantially depend on the velocity and altitude of flight, the form of a mobile object, angular orientation and flexible deformations of

a body. Even at a constant velocity of flow on the vehicle surface the vortices are generated. It results in the composite and time-varying distribution pattern of local loads on a surface of object. At high speeds of flight there are local spikes of pressure in the separate parts of vehicle. For their modeling it is important to define zones of the applying of large local loads and their time history. Usually these zones are arranged close to transitions from conical to cylindrical surface forms or to places of joints of surfaces with more composite form. In designing of vehicle the aim to avoid such connections is usually set, but it is not possible to remove them completely. Here the models for description of the most typical local loads from vortices are resulted.

Large local loads arise near to junctions of separate structural members. Usually these are places of transition from a conic surface to cylindrical, places of connection of cylinders of miscellaneous diameter. Vortex flows will be produced a little bit below streamwise places of details bonding, intensity of vortexes and frequency of their separation largely depends on conditions of flight. More particularly these models are described in [7,8].

Distributed and integral aerodynamics forces are calculated in this program block. Parameters of vehicle motion as rigid body and bending oscillations for each flight moment are taken into account. Distributed coefficients are evaluated for each point along the longitudinal axis of vehicle.

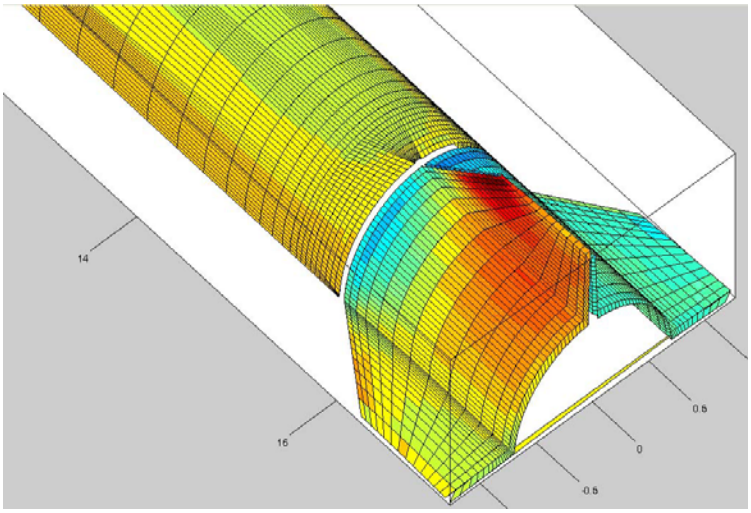

The described approach allows to calculate distributed pressure on the surface of the vehicle. Visualization of the results of calculations of the pressure for nonsymmetrical flow in the processes of flight is shown in Fig. 1.

Fig. 1 - Visualization of the nonsymmetrical pressure of the flow in the processes of flight.

4 Structure of control system

In the design stage the state-space model reduction for stabilization and guidance systems is used. The complexity of the models used in describing the aeroelastic effects via the equations of motion discussed previously makes design of stabilization and guidance systems an extremely difficult problem.

To start this process it is necessary to linearize the system dynamics near the nominal trajectory. Reduction of the linear model is then performed and the desired manner in which the reduced-order linear model approximates the full-order model.

At the stage of control system synthesis it is important to represent accurately the system frequency response in the passband of the closed loop system. There are frequencies both above and below the critical frequency range which may not need to be well modeled. The frequency range of interest is very important for applying model simplification.

There are many methods by which the linear elastic vehicle models can be simplified. Several of these methods are used in the software package. The purpose of these simplifications is to design the robust controller. Truncation deletes some of the modes or states from the full-order model. Balanced reduction minimizes frequency response error and has the certain advantages associated with obtaining the desired accuracy. Symbolic simplification addresses the impact of various physical parameters on the system responses and ignores those ones that have a little influence. Some advantages and disadvantages for each of these methods exist. After designing the robust or adaptive controller for simplified model, the analysis of real accuracy with wholeness is executed.

6 Conclusions

The uniform mathematical model is suggested for simulation of flexible aerospace vehicle flight. It consists of some particular models describing such phenomena as solid dynamics, flexibility, aerodynamics and local loads, sloshing effects and other factors.

The approach to regulator synthesis for elastic object control is offered. The procedure of synthesis is divided into two stages. At the first stage the control law for damping of the certain flexible oscillations is synthesized. At the second stage the plant is considered as rigid and it is possible to use any known method for regulator synthesis.

References:

[1] Mishin, V.P.: *Rocket Dynamics*, (in Russian). Mashinostroenie, Moscow, 1990

[2] Dewey, H. Hodges, G. Alvin Pierce: *Introduction to structural dynamics and aeroelasticity*; Cambridge, 2002

[3] Hatch, Michael R.: *Vibration simulation using MATLAB and ANSYS*; Chapman & Hall/CRC, USA, 2001

[4] Panferov A.I., Nebylov A.V. and Brodsky, S.A.: *Theory and software for simulation of complex flexible aerospace vehicles and smart control*; Proceedings of 17th IFAC Symposium on Automatic Control in Aerospace (ASA2010), September 6-10, 2010, Nara, Japan

[5] Panferov A.I., Nebylov A.V. and Brodsky, S.A.: *Mathematical Modeling, Simulation and Control of Flexible Vehicles*; Proceedings of 17th IFAC World Congress, Seoul, 16071-16077, 2008

[6] Brodsky, S.A., A.V. Nebylov and A.I Panferov: *Mathematical models and software for flexible vehicles simulation*; Proceedings of 16th IFAC Symposium on Automatic Control in Aerospace, Oxford, vol. 2, 416 – 421, 2004

[7] Caldwell, B.D., R.W. Pratt, R. Taylor and R.D. Felton: *Aeroservoelasticity*. In: Flight control systems (Roder W. Pratt, Ed.), 2000

[8] Nebylov, A.V., A.I. Panferov and S.A. Brodsky: *Flexible aerospace vehicles simulation and nonlinear control synthesis*; Proceedings of 16th IFAC World Congress, Prague, 2005

Simplified Approach to Estimation of Flexible Space Vehicle Parameters

Sergey Brodsky, Alexander Nebylov, Alexander Panferov, International Institute for Advanced Aerospace Technologies of State University of Aerospace Instrumentation, Saint-Petersburg, Russia

The model used for the design of control systems for elastic aerospace vehicles is characterized by certain set of parameters depending on elasticity of the construction. These parameters vary during the flight and differ for each copy of the object. The initial estimation of these parameters is carried out at a design stage of the object construction with application of special software using the finite elements method. More exact estimation has to be performed during natural experiment and bench tests with a mock-up model or finished object. The final estimation of parameters of elastic object indirectly is accomplished in the course of flight with use of adaptive control and optimum estimation of the state-space vector. The proposed approach can be used at each stage and is based on use of special features of construction of the simplified models of elasticity and methods of identification of its elastic properties.

Introduction[1]

The model of aeroelastic vehicle includes the dynamic equations of solid body motions, models of flexible relative displacements of construction, actuators dynamics and the cross relations defined by aerodynamic and trust forces. Such effects as sloshing, stochastic of non-stationary aerodynamic forces may be included in the models also. The unified state-space model which can be used for solving control problems has large dimension. The state-space vector components corresponded to flexible motions and components of rigid body motions are inseparably related. The invalid control based on the inexact estimation of oscillations leads to instability of motion and can induce resonance vibrations and wreck of vehicle.

It is offered to define the elastic strain of plant under the influence of some known distributed load for definition of the distributed parameters of plant elasticity. In the capacity of spread load it is possible to consider the appeared inertial forces and the known disturbing loads acting on local masses at forced elastic vibrations of plant. The distributed inertial loads corresponding to a certain mode of the free oscillations is defined by their frequency and the shape, and also mass allocation.

[1] The work has been supported by the Russian Foundation for Basic Research under the project No. 10-08-00980-a

Plant model of flexible vehicle used for estimation

Deformation of a body results in appearance of the local attack angles and slide angles. As a result, the local forces and moments of forces arise. These forces and moments are synchronized with the changes of local angles of attack and slide. The local forces and moments are the reasons of amplification or attenuation of elastic oscillations. This phenomenon is known as aeroelasticity. At excessive development of elastic oscillations the structural failure may take place. Paying attention to these effects has a great importance at control of space stations and space probes, airplanes and other mobile objects liable to the considerable dynamic loads.

Linear time invariant model

The state-space model of object with consideration of all factors may be created by applying linearization procedure to system of all nonlinear and time-varying equations about points of calculated base trajectory. It is possible to separate the motion of object to translation and rotation and research motion in one plane and to use minimal realization of system.

The state-space model of aeroelastic object may be represented in the following matrix form:

$$\dot{\mathbf{x}} = \mathbf{A}\mathbf{x} + \mathbf{B}\mathbf{u} + \mathbf{w}, \quad (1)$$

$$\mathbf{y} = \mathbf{C}\mathbf{x} + \mathbf{D}\mathbf{u} + \mathbf{v}, \quad (2)$$

where $\mathbf{x} = col(\mathbf{x}_s, \xi)$ is a state vector that includes the solid body and actuators state parameters $\mathbf{x}_s$ and modes of oscillations ξ. The input of system contains deterministic control $\mathbf{u}$, process noise $\mathbf{w}$ and measurement noise $\mathbf{v}$. The output of system is measurement vector $\mathbf{y}$.

Elasticity equations

The discrete form of flexible forced oscillations in node displacements **q** at body axes frame is

$$\Delta\mathbf{M}\ddot{\mathbf{q}} + \Delta\Xi\dot{\mathbf{q}} + \mathbf{q} = \Delta\mathbf{f}, \quad (3)$$

where $\mathbf{M}$ is diagonal mass matrix of lumped masses m_i, Δ is the inverse stiffness symmetrical matrix and Ξ is damping symmetrical matrix, $\mathbf{f}$ is vector of lumped loads in each node. Matrix Δ is calculated while taking into account free boundaries and dynamic equilibrium conditions. It implies that the matrix Δ is singular, and pair of singular values corresponds to linear displacement and rotation of vehicle as solid body. In other words, the matrix ignores the part of distributed loads which does not cause the deformation. The solution of homogeneous ordinary differential equation

$$\Delta\mathbf{M}\ddot{\mathbf{q}} + \mathbf{q} = \mathbf{0}, \quad (4)$$

without damping $\Xi = 0$, corresponds to free oscillations with natural frequencies ω_i, and mass normalized shapes $\varphi^{\langle j \rangle} = \{\Phi_{i,j}\}$, as columns of matrix Φ in the following Eigen value problem for symmetrical matrix:

$$\mathbf{M}^{1/2}\Delta\mathbf{M}^{1/2}\left(\mathbf{M}^{1/2}\Phi\right) = \left(\mathbf{M}^{1/2}\Phi\right)\Lambda, \quad \left(\mathbf{M}^{1/2}\Phi\right)'\left(\mathbf{M}^{1/2}\Phi\right) = \mathbf{E}, \quad (5)$$

$$\mathbf{\Omega} = diag\left[\omega_i\right] = \mathbf{\Lambda}^{-1/2} = diag\left[\lambda_i^{-1/2}\right]. \quad (6)$$

The dimension of equation is defined by the number of node points. The displacements of forced flexible oscillations can be represented as linear combination of shapes of free oscillations. The components of vector ξ are known as modes of flexible oscillations (generalized coordinates).

$$\mathbf{q} = \Phi\xi. \quad (7)$$

Appropriate form of flexible forced oscillations in flexible modes is

$$\Phi'\mathbf{M}\Phi\ddot{\xi} + \Phi'\Xi\Phi\dot{\xi} + \Omega^2\Phi'\mathbf{M}\Phi\xi = \Phi'\mathbf{f}. \quad (8)$$

The diagonal elements M_i of $\Phi'\mathbf{M}\Phi$ are known as general masses and the components of vector $\Phi'\mathbf{f}$ are known as general forces. In common case the matrix of general masses is diagonal, but for mass-normalized shapes (5) it is an identity matrix. The transformed damping matrix is approximately assumed as diagonal with elements equal to

$$\Phi'\Xi\Phi = diag(2\zeta_i M_i \omega_i). \quad (9)$$

The virtual stiffness and mass properties identifications

Elastic object can be considered as the system of material points, concentrated masses of those accomplish small fluctuations relative to position of equilibrium.

Then displacement q_i, points of rod under the action of the system of the concentrated forces f_j, applied at points x_j, are determined by the formula

$$q_i = \sum_{j=1}^{k} \Delta_{ij} f_j, \quad \mathbf{q} = \Delta\mathbf{f}, , \quad (10)$$

where Δ_{ij} is the influence coefficients, equal to the generalized displacement of point *i* under the action of the generalized unit power, applied at point *j*. Matrix Δ is symmetrical positively determined, and in the case for the elastic rod it is oscillatory.

The purpose is not the identification of the real parameters of mass and rigidity of all elements of the construction and not material identification. The model of the distributed elasticity selected for the identification must correspond to forms and frequencies of the prevailing harmonics, which are considered in the model of object in the state space (1), (2). The real construction can be considered as consisting of

beams, plates and shells, for which there is a direct relationship between curvature and bending strain.

For the elastic objects with the longitudinal axis of symmetry the model of thin elastic rod with the free ends proves to be sufficient in many instances. Also the lattices, formed from the elastic rods, can be examined as the simplified models of plates and shells. Unlike traditional finite beam elements, each nodal point has the transversal beam deflection as the only degree of freedom (no rotational degrees of freedom).

The following approach allowing calculation of static deflection of thin inhomogeneous beams with known arbitrary distribution of mass and stiffness under the distributed loads can be used for solving of inverse problem of identification for experimentally measured resonance frequencies and their associated mode shapes.

Model of free-free beam with arbitrary distributed stiffness and mass values

The differential equation for the transversal deflections is:

$$\frac{d^2}{dx^2}(EJ\frac{d^2q(x)}{dx^2}) = f(x). \quad (11)$$

Here variable $q(x)$ is the local beam deflection, x is the independent spatial variable, E is the Young's modulus, J is the moment of inertia of the beam's cross section and $f(x)$ is the distributed loads. The product EJ is called the flexural beam rigidity and its value can be an arbitrary function of the independent variable x. The curvature $\sigma(x) = \partial^2 q / \partial x^2$ and slope $\varphi(x) = \partial q / \partial x$ are derivatives of deflection $q(x)$ of beam.

Theory of elasticity provides the following relation between the bending moment $M(x)$ and static deflection $q(x)$:

$$EJ\frac{d^2q(x)}{dx^2} = M(x), \quad (12)$$

where the bending moment $M(x)$ can be found by integration of the transverse shear force:

$$M(x) = \int_0^x F(\varsigma)d\varsigma \text{ and } F(x) = \int_0^x f(\varsigma)d\varsigma. \quad (13)$$

The numerical procedure of calculation of curvature $\sigma_i = \sigma(x_i)$, slope $\varphi_i = \varphi(x_i)$, deflection $q_i = q(x_i)$ in nodes x_i and also calculation of influence coefficients Δ_{ij} are used further for the ***identification of the lumped masses and local rigidity.*** For *N* of points the independent indices take the following values

$$i = 1\ldots N;\ j = 1\ldots N;\ k = 1\ldots N-1;\ s = 1\ldots N-1;\ p = 1\ldots N-2;\ q = 1\ldots N-2. \quad (14)$$

For the definition of elastic displacements the basic action must not lead to the motion of object as the rigid body: progressive and rotating. The static basis of forces $\mathbf{F} = \{f_{i,j}\}$ will be determined from the conditions of equality to zero sums of forces and moments:

$$\sum_i \mathrm{F}_{i,j} = 0\,, \qquad \sum_i \mathrm{F}_{i,j}(x_i - x_1) = 0\,. \quad (15)$$

Elastic bending moments of cross sections $\boldsymbol{\mu}$ and loads applied to the nodes $\mathbf{f}$ are connected by linear transformation:

$$\mu_i = \sum_{j>i} \left(x_j - x_i\right) f_j\,, \quad (16)$$

where x is positions of nodes vector and f is loads applied to the nodes vector. In the matrix form the transformation is set by matrix $\mathbf{G}$.

$$\boldsymbol{\mu} = \mathbf{G}\mathbf{f}\,, \qquad \mathrm{G}_{i,j} = \begin{cases} x_j - x_i & (j > i) \\ 0 & (j \le i) \end{cases}. \quad (17)$$

The curvature $\boldsymbol{\sigma}$ is connected with the value $\zeta_k = \left(ej_k\right)^{-1}$ by linear transformation with the matrix $\mathbf{U}$, which components depend on the bending moment:

$$\boldsymbol{\sigma} = \mathbf{U}\boldsymbol{\zeta}\,, \qquad \mathrm{U}_{s+1,k} = \begin{cases} \mu_{k+1} & (s = k) \\ 0 & (s \ne k) \end{cases}. \quad (18)$$

Angle of tangential inclination $\boldsymbol{\varphi}$ is determined by the matrix $\mathbf{D}$

$$\boldsymbol{\varphi} = \mathbf{D}\boldsymbol{\zeta}\,, \qquad \mathrm{D}_{s+1,k} = \begin{cases} \dfrac{\mu_{k+1} + \mu_k}{2} \cdot \Delta x_k & (s+1 > k) \\ 0 & (s+1 \le k) \end{cases}, \Delta x_k = x_{k+1} - x_k \quad (19)$$

More complex structure has a matrix $\mathbf{R}$ that determines the sagging $\mathbf{q_o}$ depending on the distributed rigidity.

$$\mathrm{R}_{i,k} = \begin{cases} \dfrac{\mu_{k+1} + 2\mu_k}{6} \cdot \Delta x_k{}^2 + \sum\limits_{s}^{k<s<i} \Delta x_s \Delta x_k \dfrac{\mu_{k+1} + \mu_k}{2} & (i > k) \\ \sum\limits_{s}^{k<s<i} \Delta x_s \Delta x_k \dfrac{\mu_{k+1} + \mu_k}{2} & (i \le k) \end{cases} \quad (20)$$

The bending deflection in the cantilever frame is

$$\mathbf{q_o} = \mathbf{R}\,\boldsymbol{\zeta}\,. \quad (21)$$

Relations between bending moments and lateral displacements are the following:

$$\mathrm{q}_{oi} = \sum_{k<i} \left(\begin{array}{l} \dfrac{\left(\mu_{k+1} + 2\,\mu_k\right)}{6} \cdot \dfrac{\left(x_{k+1} - x_k\right)^2}{E_k J_k} + \ldots \\ + \dfrac{\left(x_{k+1} - x_k\right)}{2} \sum\limits_{s<k} \left(\mu_{s+1} + \mu_s\right) \cdot \dfrac{\left(x_{s+1} - x_s\right)}{E_s J_s} \end{array} \right) \quad (22)$$

The system of material points in question must satisfy the conditions of the dynamic equilibrium:

$$\sum_i \mathrm{m}_i \, \mathrm{q}_i = 0 , \qquad \sum_i \mathrm{m}_i \, \mathrm{x}_i \mathrm{q}_i = 0 . \quad (23)$$

The normal deviations from longitudinal axis $\mathbf{q}$, in the connected frame, taking into account dynamic equilibrium conditions, are correlated with bending deflection $\mathbf{q_o}$ in the cantilever frame by applying the coordinate transformation $\mathbf{T}$:

$$\mathbf{q} = \mathbf{T} \, \mathbf{q_o} , \quad (24)$$

where

$$\mathbf{T} = \mathbf{E} - \begin{bmatrix} x_1 & 1 \\ \vdots & \vdots \\ x_N & 1 \end{bmatrix} \begin{bmatrix} \sum m_i x_i & \sum m_i \\ \sum m_i x_i^2 & \sum m_i x_i \end{bmatrix} \begin{bmatrix} m_1 & m_1 x_1 \\ \vdots & \vdots \\ m_N & m_N x_N \end{bmatrix}' , \quad (25)$$

Matrix of influence coefficients for an arbitrary free-free beam, eigen frequencies and shapes

Let us determine sagging of the beam $\mathbf{q} = \mathbf{Q}^{\langle i \rangle}, \ \mathrm{i} = 1..N-2$ taking into account dynamic equilibrium under the action of the basic static disturbances $\mathbf{F}^{\langle i \rangle}, \ \mathrm{i} = 1..N-2$ and the disturbances leading to the longitudinal and rotary motion of object as solid body $\mathrm{F}_{i,N-1} = \mathrm{m}_i; \ \mathrm{F}_{i,N} = \mathrm{m}_i \, x_i .$

Let us define displacements in the body coordinate system for the rigid body:

$$\mathrm{Q}_{i,N-1} = 0; \ \mathrm{Q}_{i,N} = 0. \quad (26)$$

Then the matrix of influence coefficients will be determined as follows:

$$\mathbf{\Delta} = \mathbf{Q} \cdot \mathbf{F}^{-1} \quad (27)$$

The natural frequency ω_i, and mass normalized shapes $\boldsymbol{\varphi} = \mathbf{\Phi}^{\langle i \rangle}$ can be calculated by using (5,6).

As the basis of forces it is possible to use the random distributed actions, calibrated taking into account the conditions of dynamic equilibrium.

Simplified approach to parameters identification of elasticity and mass of beam model

The obtained linear elastic stress-strain relations can be presented by the following linear forms:

$$\mathbf{q} = L(\mathbf{f}) \, \boldsymbol{\zeta} , \ \mathbf{q} = L(\boldsymbol{\zeta}) \, \mathbf{f} , \quad (28)$$

where $L(\mathbf{f})$, $L(\boldsymbol{\zeta})$ are simply calculated matrixes.

It can be used for numerical definition of stiffness matrix. Dynamic equilibrium conditions guaranty singular filtration of local loads and separation outcome from stiffness matrix translation into solid or flexible moving. Identification of lumped mass and stiffness distributed parameters is based on these dependences also. Poly harmonic inertial loads from dominant bending oscillations can be handled as distributed local loads. The linear elastic stress-flexion (19) and stress-slope relations (18) are also used for higher reliability.

Restoration of the distributed elasticity $EJ(x)$ according to the reaction to the known distributed $\mathbf{f} = \mathbf{F}^{\langle i \rangle}$, to sagging in the cantilever coordinate $\mathbf{q}_o$, it is possible to carry out, after selecting the initial approximation of value, for the inversely proportional ζ_o:

$$\hat{\zeta} = \zeta_o + \Delta\zeta, \quad \Delta\zeta = (\mathbf{R}'\mathbf{R})^{-1}\mathbf{R}'(\mathbf{Q}^{\langle i \rangle} - \mathbf{R}\zeta_o). \quad (29)$$

However, this solution does not consider the conditions of dynamic equilibrium for the beam with the free ends, although successfully it can be used for the identification of the cantilever- fixed elements of the, for the corresponding matrix $\mathbf{R}$. The restoration of the distributed elasticity on the girder sagging by this method will contain the error of the selection of the cantilever coordinate - the error of the calculation of tangent at extreme point. Taking into account the conditions of dynamic equilibrium, the solution will take the form:

$$\Delta\zeta = (\mathbf{TR})^{+}(\mathbf{Q}^{\langle i \rangle} - \mathbf{R}\zeta_o). \quad (30)$$

The restoration of the distributed elasticity on the prevailing harmonic is based on the instantaneous position of elastic curve is determined by the equilibrium of forces of inertia and elastic. With the known mass distribution of own form, Corresponding to harmonious fluctuation with frequency ω, it can be considered as a static deflection under the influence of the forces proportional to a local deviation, to dot weight and a frequency.

$$\mathrm{f}_i = \mathrm{m}_i \mathrm{Q}_{i,j}\, \omega_j^{\,2}. \quad (31)$$

In the task of the identification of mass or rigidity, as the a priori information can be used both the information about the identified parameter and the condition of its relative invariability, last conditions smooth out estimation and are more acceptable for the systems, obtained by the discreteness of the continuous.

Conclusions

The results of performed investigations, directed toward the study of the possibilities of the identification of the model of elastic flying vehicle, are:

- special features are examined and procedures are developed for the simultaneous estimation of the state vector and identification of model of object with

the lumped parameters, and the correction of the basis of its own forms in the model of the measurements;

- the problem of identification with the assigned design diagram of the distributed model of the elasticity of that corresponding to the prevailing harmonics is analytically solved;
- it is proposed to consider unidentified elastic forms of the fluctuations of the highest frequencies as the distribution of noise along the elastic curve.

The approach for estimation of distributed parameters of elastic vehicle such as distributions of mass and stiffness can be used for estimation of other parameters of flexible construction. The sloshing effects as associated masses and additional oscillators and solid propellant burn-out as mass distributions changing can be considered as estimated properties.

The offered approach is used in the specialized program for modeling and research of a broad class of elastic plants, developed in IIAAT SUAI.

References:

[1] Brodsky S.A., A.V. Nebylov and A.I Panferov: *Mathematical models and software for flexible vehicles simulation*; Proceedings of 16th IFAC Symposium on Automatic Control in Aerospace, Oxford, 2004, Vol. 2, pp. 416 – 421

[2] Brodsky S.A., A.V. Nebylov and A.I. Panferov: *Measuring Optimization in Optimal Control of Flexible Aerospace Vehicles*; Proceedings of 17th IFAC World Congress, Seoul, 2008, pp. 13305 – 13309

[3] Caldwell B.D., R.W. Pratt, R. Taylor and R.D. Felton: *Aeroservoelasticity*; In: Flight control systems. Roder W. Pratt (Ed), 2000

[4] Dewey H., Hodges, G. Alvin Pierce: *Introduction to structural dynamics and aeroelasticity*; Cambridge, 2002

[5] Gawronski Wodek K.: *Advanced Structural Dynamics and Active Control of Structures Series*; Mechanical Engineering Series, Springer-Verlag New York, Inc., 2004

[6] Nebylov A.V., A.I. Panferov and S.A. Brodsky: *Flexible aerospace vehicles simulation and nonlinear control synthesis*; Proceedings of 16th IFAC World Congress, Prague, 2005

[7] Sol H., T. Lauwagie, P. Guillaume: *Identification of Distributed Material Properties using Measured Modal Data*; Proceedings of the International Seminar on Modal Analysis (ISMA), 2002, pp. 695-704